

Ag-Ni-Co-As-U Mineralization
In The Black Hawk Mining District,
Grant County, New Mexico

THESIS
G31a
1986
C.2

by

Jeffrey E. Gerwe



Submitted in Partial Fullfillment
of the Requirements for the Degree of
Master of Science in Geology

New Mexico Institute of Mining and Technology

Socorro, New Mexico

March, 1986

TABLE OF CONTENTS

	page
ABSTRACT	iv
ACKNOWLEDGMENTS	vi
INTRODUCTION	1
REGIONAL GEOLOGIC SETTING	3
PREVIOUS WORK	9
METHODS OF INVESTIGATION.....	10
RESULTS	12
Local Geology and Geochemistry	12
Faults and Fractures	28
Mineralization	29
Alteration Assemblages.....	33
Geochemistry of the Hydrothermally Altered Monzodiorite	39
Fluid Inclusion Study ..	40
K-Ar Dates	46
DISCUSSION	47
Pressure and Depth of Mineralization	47
Mechanism for Mineral Deposition ...	49
Age of Mineralization	50
Comparison with Other Ag-Ni-Co-As-U Type Deposits ...	52
Critical Factors for the Formation of Ag-Ni-Co-As-U Type Deposits	61
Genetic Theories	62
SUGGESTED GENETIC MODEL	66
SUMMARY AND CONCLUSIONS	70
Summary of the Geologic History in the Black Hawk District	70
Conclusions	71
APPENDICES	74
REFERENCES	81

APPENDICES

APPENDIX A: Chemical Analysis and CIPW Norm. Calc.	74
APPENDIX B: Petrologic Descriptions of Geoc. Samples.....	76
APPENDIX C: Fluid Inclusion Data	79

PLATES

1. Geologic Map of the Black Hawk district (also contains chemistry sample locations and alteration distribution) in pocket.

FIGURES

1. Location and regional geology map	2
2. Alkali vs. silica plot of the igneous rocks	15
3. A-F-M diagram of the igneous rocks	16
4. Histogram of Ni and Co analysis	20
5. Photo of precursor sulphide stage	31
6. Photo of weathered ankerite vein	32
7. Idealized diagram of the textural and mineralogical changes of the alteration	35
8. Photo of altered rock from the inferred paleoregolith	37
9. Photos of hand specimens and thin sections of the alteration assemblages	38
10. Representative sketches of the four types of fluid inclusions observed	42
11. Histograms of homogenization temperatures of fluid inclusions	44

12. Histograms of salinities of fluid inclusions	45
13. Paragenetic sequence of the Echo Bay vein, Great Bear Lake Area	57
14. Paragenetic sequence of the Black Hawk vein	58
15. Magmatically derived model for the deposition of Ag-Ni- Co-As-U type deposits	63
16. Idealized model of the ore deposition for the Black Hawk District	67
17. Pressure-temperature paths for hydrothermal fluids ...	68

TABLES

1. Geologic column for the Burro Mountains	4
2. Ore deposits of western Grant County	8
3. Typical chemical analysis of igneous rocks	13
4. Recalculated analysis of porphyritic monzodiorite gneiss	40
5. K-Ar age data	46
6. K-Ar dates for various rocks in the region	51
7. Physiochemical parameters for Ag-Ni-Co-As-U deposits ..	55

ABSTRACT

The Black Hawk mining district is one of the few occurrences of Ag-Ni-Co-As-U mineralization in the U.S.. This mineralization occurs within carbonate-filled, northeast-trending fractures hosted by Proterozoic, porphyritic monzodiorite gneiss and is spatially associated with a late Cretaceous, diorite porphyry intrusion. Analysis of both Precambrian and late Cretaceous rock-types contain anomalous amounts of cobalt and nickel; 35ppm Co, 33ppm Ni, and 20ppm Co, 11ppm Ni, respectively. Whole-rock analyses indicate that the rocks in the district are of a calcalkaline, subalkaline affinity. They also indicate that the Precambrian rocks are more alkaline than the Cretaceous rocks. Intermediate argillic and propylitic alteration assemblages are associated with vein mineralization. K/Ar dating of the intermediate argillic assemblage indicates an age of 65.3 +/- 1.2 m.y..

Fluid inclusion thermometric measurements indicate homogenization temperatures (Th) of the pre-ore stage range from 410 to 290 °C, with a majority greater than 350 °C and a salinity of 2 eq.wt.% NaCl. Fluid from this stage behaved as a supercritical fluid. Boiling is indicated for a Th of 380 °C suggesting a depth of mineralization of about 2.5 km. Samples of ankerite associated with silver mineralization yield homogenization temperatures ranging from 390 to 160

°C, averaging 220 °C and salinities of less than 6 eq.wt.% NaCl.

Similarities between the Black Hawk district and other Ag-Ni-Co-As-U districts are their occurrence within narrow, carbonate-dominated veins in Precambrian batholithic complexes; the presence of a precursor sulphide phase; silver mineralization indicated to have occurred from about 230 °C fluids; and the presence of high salinity fluid inclusions. Differences are their variable age for silver deposition ranging from Precambrian to Tertiary; depth of mineralization; and the composition of the associated intrusive with the silver veins.

The geology, geochemistry, and fluid inclusion data suggest that the Black Hawk deposit was mineralized by an epithermal system during Laramide intrusive activity, but deposition occurred at greater depths and higher temperature than has been reported for typical epithermal deposits. Metals were probably transported by chloride complexes and it is proposed that ore precipitation resulted from pH increases due to wallrock reactions.

ACKNOWLEDGMENTS

Financial support for this study was provided in part by a U.S. Bureau of Mines grant (no. G112413582-83) and in part by the New Mexico Geological Society. I thank Trevor Harder and The Black Hawk Consolidated Mining Company for access to their property.

I would like to acknowledge and thank Dr. David I. Norman for suggesting this project and for critically reviewing this manuscript. A special thanks to G.R. Osburn for his suggestions in the field and in addition to J.M. Robertson for their helpful editorial comments. In addition, I thank Babette Faris, Philip Kyle, and Lynn Branvold for their assistance with the geochemical analyses and Anne Wright for the K-Ar dating analyses. Also, I thank all my friends and colleagues for their suggestions and help; especially Kevin and Sylveen Cook for giving me a place to stay while I was finishing my thesis. Finally, I would like to thank my family and friends in Kentucky for their support and encouragement throughout my education.

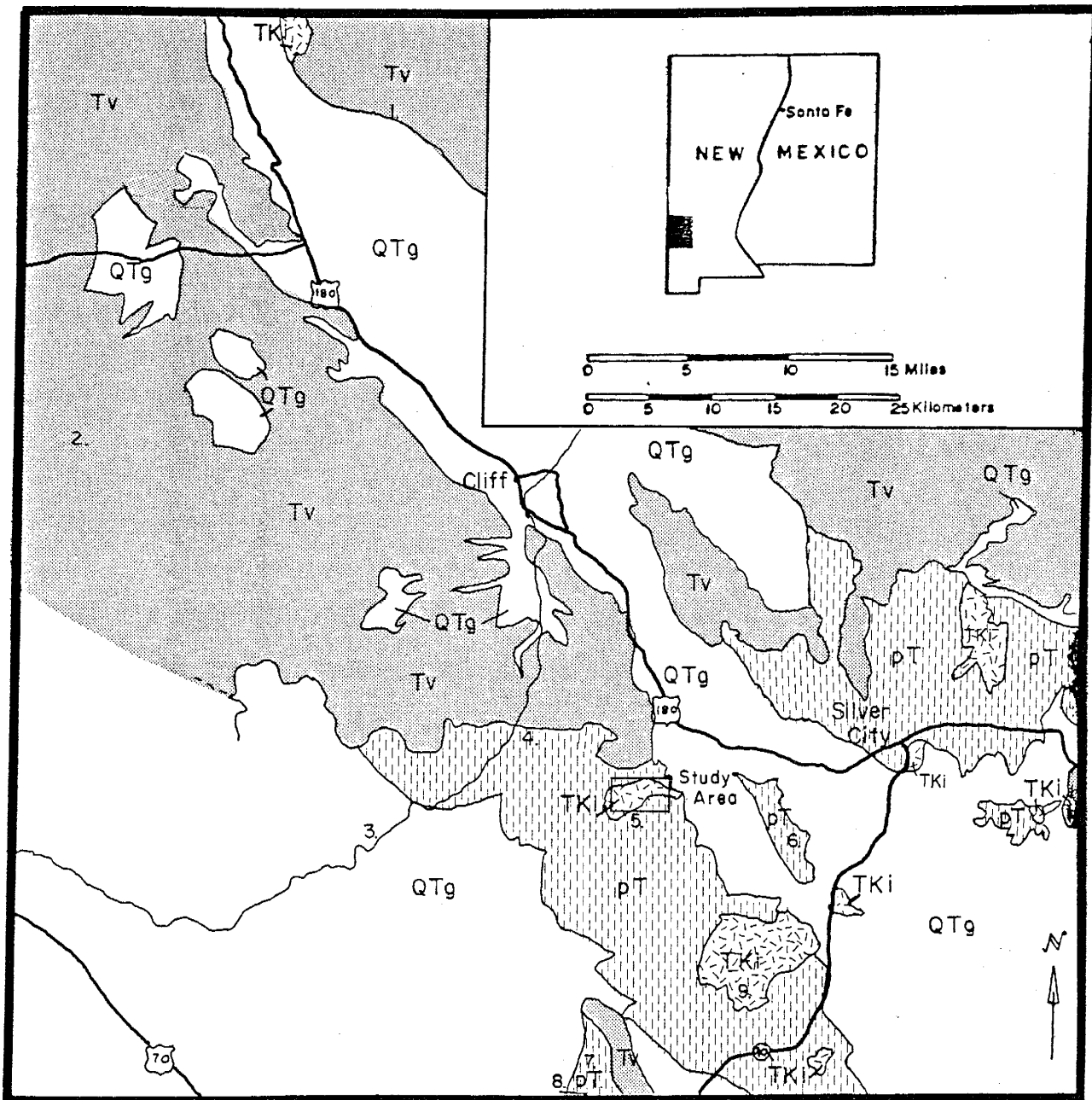
INTRODUCTION

The Black Hawk mining district contains one of the few occurrences of Ag-Ni-Co-As-U mineralization in the U.S.. It is located within the Burro Mountains, thirty-four kilometers southwest of Silver City, New Mexico (Fig. 1). Mineralization occurs as a complex suite of native silver, nickel and cobalt arsenides, and pitchblende in a carbonate-filled, fissure-vein system (Gillerman and Whitebread, 1956). The veins are largely hosted by Proterozoic, porphyritic monzodiorite gneiss and are spatially associated with a late Cretaceous, diorite-porphyry intrusion. (Gillerman and Whitebread, 1956).

The major mines located within the district are the Black Hawk, Alhambra, Rose, Silver King (Hobson), and Good Hope (Plate 1). Mineralization was first discovered in 1881 by a soldier who found silver-rich float near the Alhambra mine (Dyer, 1953). Silver production from the district prior to 1893 is estimated to have been between \$1,000,000 and \$1,500,000 (Gillerman and Whitebread, 1956). There has been no reported production since then.

Since Ag-Ni-Co-As-U deposits are of rare occurrence, the principle problem has been to determine what unique set of geologic circumstances are necessary for the formation of

Figure 1. Location and regional geology map of Black Hawk area, Grant County, New Mexico (modified after Elston et al., 1976). Deposits listed in Table 2 are approximately located here and marked by: 1, Sacaton Mesa Area; 2, Steeple Rock District; 3, Redrock Area; 4, Wild Horse Mesa; 5, Bullard Peak Area, 6, Little Burro Mountains; 7, Malone District; 8, Gold Hill District; and 9, Tyrone District.



QTg

SEDIMENTARY ROCKS (Holocene to Miocene) includes Gila Conglomerates, younger gravels and alluvium.

Tv

DATIL-MOGOLLON VOLCANIC ROCKS (Eocene to Miocene), volcanic and volcaniclastic rocks of rhyolitic to basaltic composition.

TKi

EARLY INTRUSIVE ROCKS, UNDIFFERENTIATED (Late Cretaceous to Eocene) mainly porphyritic rocks of intermediate composition.

PT

PRE-TERTIARY ROCKS, UNDIFFERENTIATED (Precambrian to Upper Cretaceous)

Precambrian igneous and metamorphic rocks and Cretaceous sedimentary and volcanic rocks.

this type of mineralization. This will only be known when knowledge of a number of like deposits can be compared in order to determine their common characteristics. Hence, the Black Hawk District was studied in order to add to the knowledge concerning these enigmatic deposits. This study included petrography, whole-rock geochemistry, detailed mapping and K-Ar dating of the alteration assemblages, and fluid inclusion analysis of vein material.

REGIONAL GEOLOGIC SETTING

The Black Hawk district occurs within the Basin and Range province along the Burro uplift and south of the Datil-Mogollon volcanic field. The Burro uplift is bounded by the Knight Peaks fault on the southwest side and the Mangas fault to the northeast (Hedlund, 1980). The stratigraphy of the Burro uplift is summarized in Table 1.

The Burro Mountain Batholith Complex is a Precambrian, northwest-trending belt of metamorphic and intrusive rocks (Fig. 1). The oldest exposed rocks in the region are members of the Bullard Peak Metamorphic Series which crop out along the crest, west flank, and north end of the Big Burro Mountains (Hewitt, 1959). This metamorphic series consists of sedimentary and igneous rocks which are regionally metamorphosed to the amphibolite facies including quartz-feldspar and sillimanite gneisses; mica schists and

Table 1. Geologic Column For The Burro Mountains, New Mexico

TIME AND ROCK UNITS		
Cenozoic Era	Quaternary	Unconsolidated gravels
	Tertiary	Gila Conglomerate, sandstone Calc-alkaline stocks and dikes
		Mogollon volcanics Basalts-andesites-rhyolites
Mesozoic Era	Cretaceous	Calc-alkaline stocks and dikes Andesite and quartz-latite flows
		Colorado Fm. shale
		Beartooth Fm. quartzite
	unconformity	
M. to L. Proterozoic	Burro Mountain Batholith Complex	
	Intrusives	Monzodiorite, granodiorite, and several types of granite
	Ash Creek Series	Cordierite, andalusite, and biotite hornfelses; phyllite and serpentine-carbonate rocks
	Bullard Peak Series	Quartz-feldspar and sillimanite gneisses; mica schists and gneisses; hornblende gneiss and amphibolite

gneisses; hornblende gneiss; and amphibolites (Hewitt, 1959). Hedlund and Stacey (1983) reported an average U/Pb age of 1550 m.y. from zircon for a biotite gneiss from the Bullard Peak Series. This age should be interpreted as a minimum estimate.

Hewitt (1959) interprets the Ash Creek Metamorphic Series to be the second oldest rocks in the region and describes them as complex xenoliths or roof pendants in the Burro Mountain granite. This series consists of cordierite, andalusite, and biotite hornfelses, phyllites, and serpentine-carbonate rocks. Hewitt suggests these rocks were originally sediments that were subjected to regional metamorphism to the greenschist facies and to several contact metamorphic events.

Plutonic rocks of the Burro Mountain Batholith Complex consist primarily of a heterogeneous granite, but also include a large mass of porphyritic monzodiorite gneiss and several small isolated masses of anorthosite, diabase, diorite, and syenite (Gillerman, 1964). Hedlund and Stacey reported a U/Pb age of 1445 +/- 10 m.y. from zircon for the granites and Hedlund (1980) reported a K-Ar age of 1380 +/- 45 m.y. from biotite for the porphyritic monzodiorite gneiss. The Black Hawk district is situated mainly in this gneiss.

The Burro Mountain Batholith Complex is unconformably overlain by the lower Cretaceous, Beartooth Formation that consists of a fine-grained, quartz arenite interlayered by thin shale beds and having a hematite-stained, pebbly, cherty conglomerate base (Table 1). The Beartooth Formation is conformably overlain by the Colorado Formation that consists of a black carbonaceous shale. These shales are found overlain by Cretaceous andesites and quartz latites in some areas and unconformably overlain by Tertiary volcanics in others (Gillerman, 1964). Two major Laramide stocks, which are the Twin Peaks diorite porphyry stock located on the west boundary of the Black Hawk district and the Tyrone quartz monzonite intrusion located 10 kilometers southeast of the Black Hawk district, intrude the Burro Mountain Complex and whose published ages are 72.5 +/- 7m.y. and 56.2 +/- 1.7m.y. (Hedlund, 1980), respectively.

The northern portion of the region is covered by Tertiary volcanic and volcanoclastic rocks of the Datil-Mogollon volcanic field. Their composition ranges from basalts to andesites to rhyolites. One of the major units which occurs just north of the Black Hawk district is the Tadpole Ridge Quartz Latite which has been dated at 31.2 m.y. (Elston and Northrop, 1976).

Gila Conglomerate consisting of conglomerates and interbedded sandstones unconformably overlies pre-Tertiary and some Tertiary rock units and is conformable with others (Gillerman, 1964). It is unconformably overlain by Quaternary gravels and bolson deposits (Gillerman, 1964).

Mineral occurrences surrounding the Black Hawk district are numerous. They range in age from Precambrian to Tertiary and consist of metamorphic W-Bi-Mo deposits, porphyry copper deposits, and base and precious-metal vein deposits (Fig. 1 and Table 2). The oldest mineralization occurs just south of the study area in the Bullard Peak district. This mineralization consists of W, Bi, Mo, and tourmaline in amphibolite xenoliths and pegmatites within the Burro Mountain granite. Sheelite is the primary mineral. The Tyrone porphyry copper deposit, which is part of the Laramide porphyry copper belt (80-45 m.y.) of the southern Cordilleran, is associated with several plutons that are suggested to be subvolcanic (Stacey and Hedlund, 1983). Primary minerals are pyrite, chalcopyrite, sphalerite, molybdenite, quartz, and fluorite. Chalcocite is the principal ore mineral and is supergene in origin. Sericite, quartz, chlorite, epidote, and kaolinite are common alteration products in the host rocks. Within 25 kilometers of the Black Hawk are 5 base and precious metal vein deposits (Fig. 1) that occur in east-northeast

Table 2. Ore deposits of Western Grant County

Age	District	Type	Description
Precambrian			
	Bullard Peak	Metamorphic	W, Bi, Mo, and tourmaline in amphibolite xenoliths and pegmatites within Burro Mountain granite
	Redrock area	Metamorphic	Ricolite (serpentine), asbestos, and magnetite in Ash Creek Metamorphic Series
Laramide			
	Tyrone	Porphyry copper	Supergene enriched copper along with minor precious metals in a quartz-monzonite stock
	Redrock area	Hydrothermal vein	Ag, Cu, Pb, Zn in Burro Mountain granite and Beartooth quartzite
	Little Burro Mountains	Hydrothermal vein	Au, Ag, and base metals in monzonite porphyry and Beartooth quartzite
	Wild Horse	Hydrothermal vein	U-quartz and base metal sulfides in Burro Mt. granite and Beartooth quartzite
	Malone	Hydrothermal vein	Au, Ag, and minor base metals in rhyolite tuffs and Burro Mt. granite
	Gold Hill	Hydrothermal vein	Au, Ag, and minor base metals in Burro Mt. granite
Tertiary			
	Steeple Rock	Epithermal vein	Au, Ag, and base metals in andesite and latite
	Sacaton Mesa area	Epithermal vein	Au-tellurium in andesite and latite

Data taken from Gillerman (1964).

trending faults in Cretaceous volcanic or sedimentary rocks and the Burro Mountain granite (Gillerman, 1964). This E-NE trend of faults, fissure veins, and dikes is typical of Laramide tectonics (Heidrick and Titley, 1982). North of the Black Hawk are Steeple Rock and Sacaton Mesa epithermal base and precious metal deposits (Fig. 1) that occur in Tertiary volcanics. They both appear to be associated with ring-fractures and moat deposits of an unnamed caldera (Elston and Northrup, 1976).

PREVIOUS WORK

Lindgren (1910) and A.A. Leach (1916) first studied the geology and mineralization of the district and described the production of the major mines. Gillerman and Whitebread (1956) studied the U-Ni-Co-Ag mineral deposits and mapped in detail a six and a half square kilometer area in the Black Hawk district.

Von Bargen (1979) did a detailed study of the mineralization of the Black Hawk district and surroundings. Von Bargen determined the following paragenesis based on polished section, thin section, and microprobe analysis. There is a pre-ore stage of pyrite and pyrrhotite as fracture fill and disseminations in the wallrock. This is followed by three stages of ore mineralization: stage 1 is pitchblende + Ni and Co arsenides + native silver; stage 2 is base metal sulfides + argentite; stage 3 is native

silver + Cu sulfides and sulfarsenides. Very little, if any, gold is present. Von Bargen documented the chemical environment of deposition of the ores based on mineral equilibria. Briefly summarized, he concluded that the environment of ore deposition had the following characteristics: (1) ore precipitated at the temperatures between 350 and 50 degree Celsius; (2) ores were deposited at a depth of 600 to 900 meters (2000 to 3000ft) below the contemporaneous surface at fluid pressures between 100 and 200 bars; (3) the pH of the solution varied between 4.5 and 5.6; (4) $\log fS_2$ varied between -20 and -15; and (5) $\log fO_2$ decreased from -42 to -50 during mineralization.

METHODS OF INVESTIGATION

The field work for this investigation consisted of mapping the alteration and sampling for chemistry, fluid inclusion, and K-Ar dating analysis of the host rock and mineralization. During this investigation, Gillerman and Whitebread's (1956) detailed geologic map of the Black Hawk mining district was used as a base map, but the lithologies have been described and reclassified according to Streckeisen's (1973) classification scheme based on modal mineral composition.

Forty thin sections were prepared and studied to characterize the geology and alteration of the district. Plagioclase compositions were determined by the Michel-Levy method as described in Kerr(1977). Twenty-nine whole-rock samples were analyzed for major elements by X-ray fluorescence (XRF) spectrometry using the fusion-disk techniques of Norrish and Hutton (1969). Three samples of porphyritic-monzodiorite gneiss and two samples of diorite porphyry were analyzed for their nickel and cobalt concentrations using atomic absorption (AA) techniques as described by Branvold (1974). CIPW normative minerals were calculated from the major element data using standard methods (Cox, 1979). A total of twenty-five doubly polished thick sections of quartz, dolomite, and sphalerite were prepared for fluid inclusion analysis. Homogenization temperatures (Th) and salinity measurements were determined by microscopic observations using standard methods (Roedder, 1972). Mafic minerals in the rock hosting the vein and the intermediate-argillic vein alteration were dated by K-Ar methods at Ohio State University, Columbus, Ohio by Anne Wright.

RESULTS

Local Geology and Geochemistry

Thirteen rock types have been recognized in the Black Hawk district (Gillerman and Whitebread, 1956). Field observations indicated that the geologic contacts were well mapped, however, it was apparent that the rocks could be better named. Therefore, the author used Gillerman and Whitebread's map as a base (Plate 1) leaving the geologic contacts unchanged while changing the their rock names to new names based on petrographic studies using the rock classification and nomenclature recommended by the IUGS subcommission on the systematics of igneous rocks (Streckieson, 1973). Also in some cases chemical analyses showed the field names to be incorrect.

Chemical analyses and CIPW normative minerals of the Black Hawk rock suite are given in Appendix A. For comparison, typical analyses from this study are presented with average chemical compositions of similiarly named rocks in Table 3. The chemical variations in the analysis for individual rock types are not large and may be due to minor alteration of the samples seen in thin section as a slight sericitization of plagioclase feldspars and chloritization of biotite (Appendix B).

TABLE 3. Typical analyses of rocks in the Black Hawk District compared to average values of rocks given the same field name.

Major oxides (wt.%)	Monzodiorite		Diorite		Syenite		Granite		Diabase		Rhyolite		Granodiorite		Andesite				
	1	2	3	4	5	6	7	8	9	10	11	12	13	14	15	16	17	18	19
SiO ₂	53.41	56.14	55.01	59.54	49.65	65.12	58.67	68.69	59.85	76.1	71.86	48.24	50.43	78.65	73.96	64.91	66.09	59.5	59.02
TiO ₂	.96	1.52	1.1	1.11	1.19	.43	.97	.44	.86	.05	.31	1.53	1.89	.1	.28	.69	.54	.7	.89
Al ₂ O ₃	16.65	18.19	16.79	17.1	16.43	17.18	17.01	14.63	17	12.96	14.43	17.1	16.13	14.97	13.48	16.67	15.73	16.68	17.34
Fe ₂ O ₃	8.5	8.69	8.37	6.22	10.82	4.61	7.02	3.5	5.92	1.2	2.84	12.21	10.28	2.06	2.61	5.09	4.11	5.9	6.9
MnO	.15	.17	.15	.16	.18	.13	.12	.01	.13	.08	.05	.19	.21	.05	.06	.07	.08	.11	.14
MgO	6.41	2.73	6.2	2.63	9.55	1.31	3.79	0	1.91	.15	.72	7.27	6.9	.36	.4	1.82	1.74	2.79	3.39
CaO	8.01	5.27	6.37	5.08	7.89	5.15	6.72	.26	3.61	.47	1.86	9.73	9.7	.09	1.16	3.63	3.83	7.88	6.92
Na ₂ O	3.45	4.16	3.2	4.45	2.87	3.62	3.6	.24	5.35	3.45	3.71	2.24	2.98	.37	3.6	3.34	3.75	3.73	3.55
K ₂ O	2.27	2.72	2.64	3.29	1.26	2.2	1.8	12.1	5.07	5.37	4.1	1.23	1.13	4.09	4.37	3.57	2.73	2.49	1.65
P ₂ O ₅	.25	.41	.2	.42	.19	.26	.3	.13	.3	.05	.12	.3	.36	.02	.07	.22	.18	.23	.21
TOTAL	100	100	100	100	100	100	100	100	100	100	100	100	100	100	100	100	100	100	100

NOTE: Values recalculated to 100% w/o H₂O. Analyses: 1- fine-grained monzodiorite; 2- porphyritic monzodiorite; 3- biotite monzodiorite; 4- avg. monzodiorite (from Le Maitre); 5-diorite; 6-diorite porphyry; 7-avg. diorite (from Le Maitre); 8-syenite; 9-avg. syenite (from Le Maitre); 10- granite; 11-avg. granite (from Le Maitre); 12-diabase; 13-avg. diabase (from Le Maitre); 14-rhyolite; 15-avg. rhyolite (from Le Maitre); 16-granodiorite; 17-avg. granodiorite (from Le Maitre); 18-andesite; 19-avg. andesite (from Le Maitre). Original analyses are in appendix A.

An alkali-silica diagram (Fig. 2) is used to classify the rocks chemically. The IUGS modal classification and the chemistry scheme (Fig. 2) are in agreement except for the diorite and diorite porphyry. These exceptions are discussed below in the individual rock descriptions. Reasons why the rock names used in this study are based on modal compositions even though a chemistry scheme is presented are that the majority of the rocks are medium to coarse grained thus allowing the mineralogy to be easily identified in thin section and since so many of the rocks are Precambrian and occur in an area which has been subjected to hydrothermal fluids, it is possible that their chemistry has been altered thus making classification based on rock chemistry unreliable.

In general, the Black Hawk rocks are indicated to be subalkaline (Fig. 2). There is a trend of higher alkalinity for the Precambrian rocks compared to the younger Cretaceous rocks. When the data are plotted on an A-F-M diagram (Fig. 3), they indicate that the rocks are calc-alkaline. However, because the Precambrian rocks are not pristine, these interpretations should be viewed with caution.

Figure 2. Alkali-Silica diagram for igneous rocks in the Black Hawk district (+ = Precambrian rocks, ♦ = Cretaceous rocks). Rock classification scheme modified after Cox (1978). Subalkaline and alkaline field dividing line from Irvine and Baragar (1971).

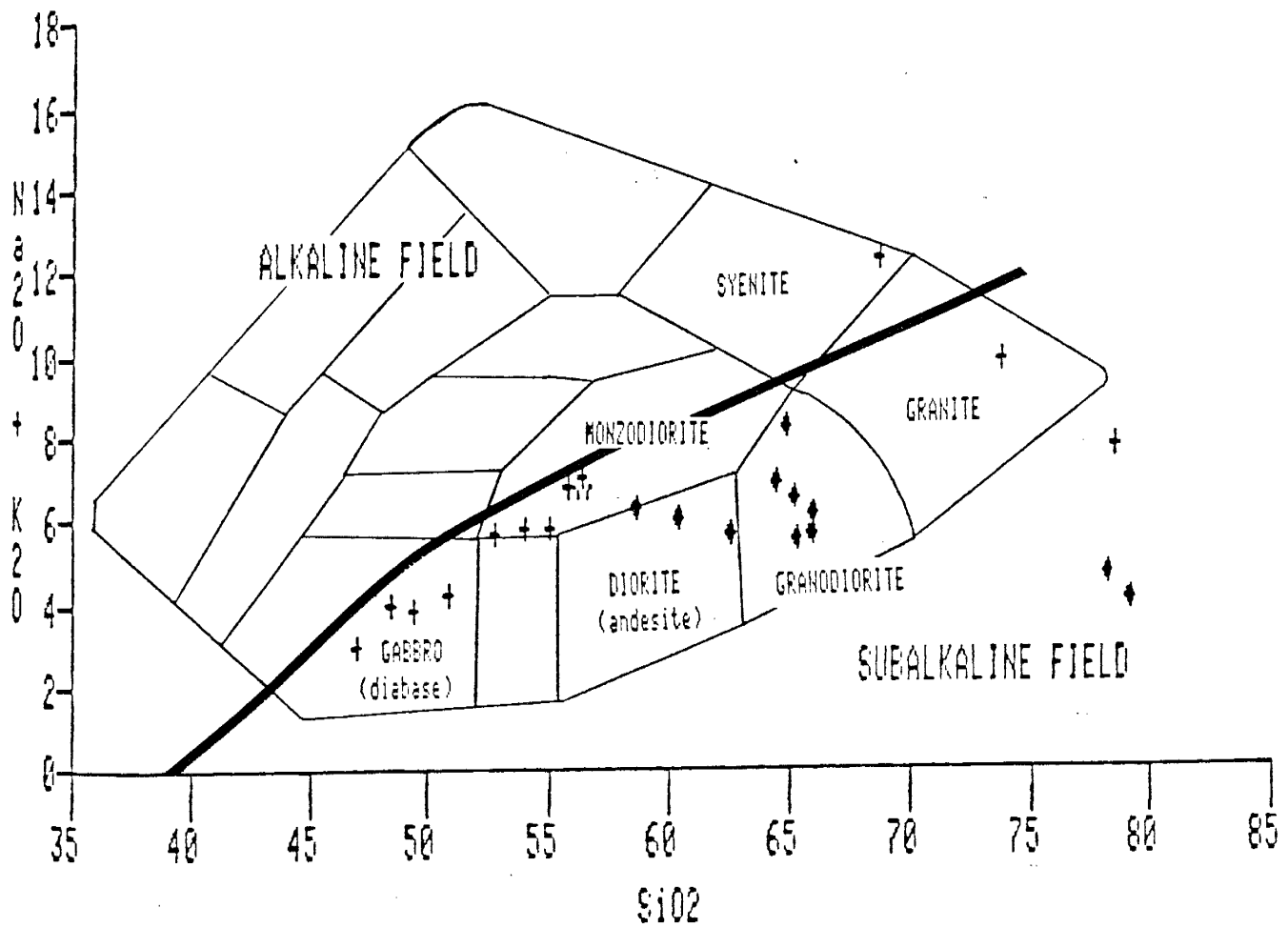
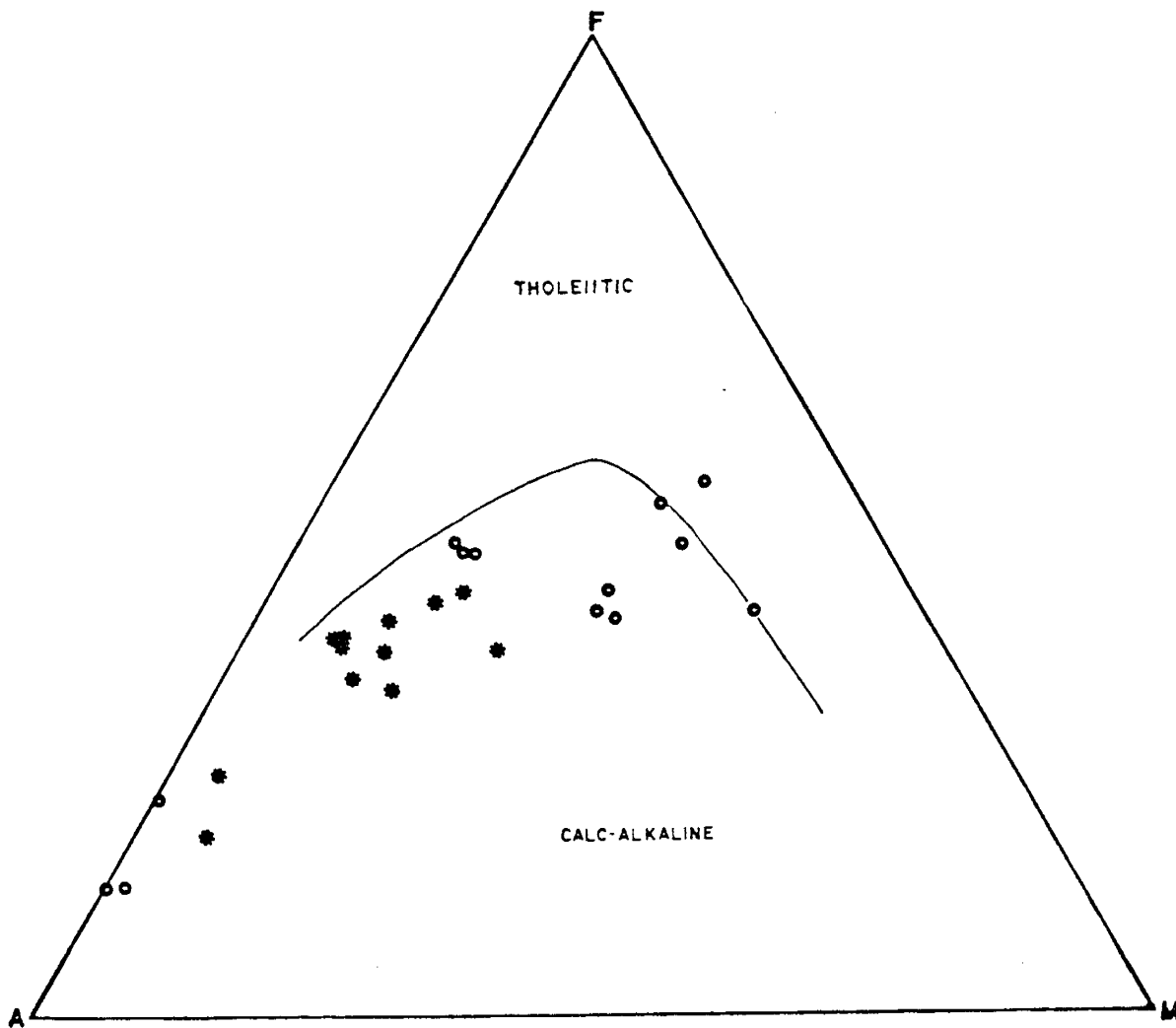


Figure 3. A-F-M diagram for igneous rocks from the Black Hawk district (after Irvine and Baragar, 1971; ● = Precambrian rocks, * = Cretaceous rocks).



PRECAMBRIAN LITHOLOGIES

Feldspathic quartzite and schist (Bullard Peak Series; Hewitt, 1959)

Feldspathic quartzite and schist comprise approximately 3% of the rocks in the Black Hawk district as two irregular masses. The quartzites are interbedded with schist and are intruded by granite, diorite, and Twin Peaks diorite porphyry. The quartzite is gray to buff, fine to medium grained (.5-2mm), and composed of quartz(50-60%), feldspar(25-30%) and minor mica (5-10%) and magnetite(1-2%). The schist is tightly folded, foliated, medium-grained (2-4mm), and composed of mica(70-80%) , quartz(10-20%), and magnetite(1-2%). Both contain 1-2mm veinlets of epidote, weather to a reddish brown color, and typically form ridges.

Fine-grained monzodiorite

Fine-grained (<1mm) monzodiorite occurs in the southeastern part of the district as small, irregular, north-northeasterly trending masses. This unit comprises 4% of the district and characteristically weathers to a reddish-gray color. Gillerman and Whitebread's (1956) name for this unit is fine-grained quartz diorite.

The fine-grained monzodiorite is hypidiomorphic-granular and consists of plagioclase (50-60%), biotite (5-10%), hornblende (10-15%), potassium feldspar (10-15%), quartz (0-5%) and trace amounts of apatite, sphene, sericite, and iron oxides. Plagioclase (An28-31) crystals are as large as 5mm but typically .2-.5mm, slightly sericitized, anhedral, and some of the plagioclase crystals are broken and rimmed by more plagioclase. Subhedral (.3-.5mm), light-brown biotite and blue-green hornblende are intergrown. Generally the biotite has bent cleavage planes. This monzodiorite is primarily higher in Fe_2O_3 , MgO, and CaO and lower in SiO_2 , Na_2O , and K_2O than an average monzodiorite (Table 3).

Porphyritic monzodiorite gneiss

Porphyritic monzodiorite gneiss is medium-gray, medium to coarse-grained, and comprises 65% of the Black Hawk district. The best exposures occur 500 meters south of the Black Hawk mine in Black Hawk Canyon and 800 meters southeast of the same mine in Dale Canyon Creek. This monzodiorite is intruded by pegmatites and aplite dikes in the southern portion of the district, while the dikes are less abundant in the north. This unit characteristically weathers to a reddish-brown, crumbly or knobby surface. Foliation is evident in outcrop scale by the orientation of the porphyritic feldspars. Gillerman and Whitebread's

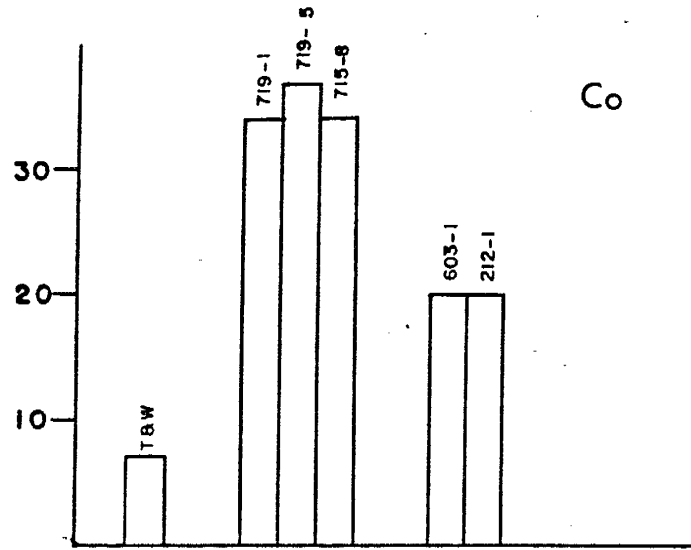
(1956) name for this unit is porphyritic quartz diorite gneiss.

This porphyritic monzodiorite gneiss is hypidiomorphic-granular. The major constituents are white to pink plagioclase feldspar (60-65%), potassium feldspar (10-15%), biotite (5-12%), hornblende (5-15%), quartz (2-5%), iron oxides (2-5%), and apatite (1-2%). Anhedral to subhedral plagioclase has an average composition of An 31 (andesine), is albite and pericline twinned with occasional normal zoning, has myrmekitic intergrowth along plagioclase-quartz grain boundaries, and commonly contain bent twin lamellae. Sericitic alteration occurs along twin lamellae. Anhedral orthoclase is interstitial to other minerals. Plagioclase feldspar phenocrysts are as large as 5 cm but typically 2-3 cm. Yellowish-brown biotite is commonly intergrown with blue-green hornblende. The biotite is commonly crenulated. The hornblende ordinarily contains poikilitic apatite euhedra and magnetite. The mafic minerals altered to chlorite.

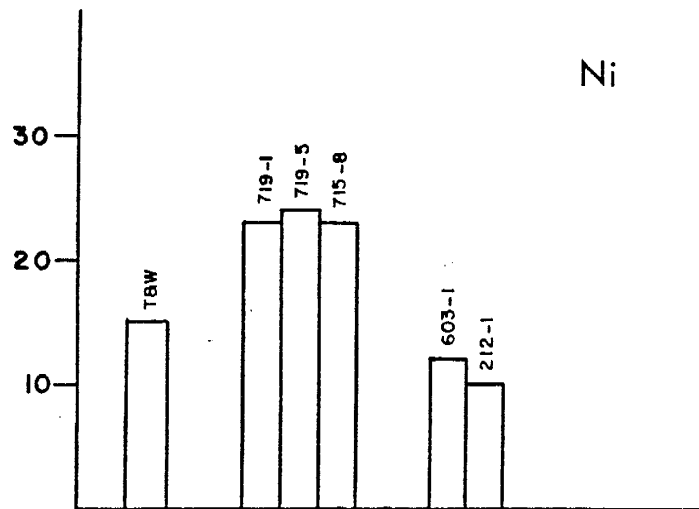
Porphyritic monzodiorite gneiss is similar to an average monzodiorite except it is higher in Al_2O_3 and Fe_2O_3 and lower in SiO_2 . Three porphyritic monzodiorite gneiss samples (Appendix A) exhibit higher Co and Ni values compared to an average intermediate igneous rock (Fig. 4).

Figure 4. Histogram of Ni and Co analysis from the Black Hawk district. T and W = average intermediate igneous rocks from Turekian and Wedepohl, 1961; 719-1, 719-5, and 715-8 are Proterozoic porphyritic- monzodiorite gneiss; 603-1 and 212-1 are Cretaceous diorite porphyry.

CONCENTRATION(ppm)



Co



Ni

Biotite monzodiorite

Small, northwest trending masses of black, medium-grained, equigranular, biotite monzodiorite comprise about 1% of the rocks in the district. Exposures of this unit occur in the southern portion of the district. This monzodiorite is similar to the porphyritic monzodiorite gneiss except it lacks porphyritic feldspars and is richer in biotite and hornblende. Gillerman and Whitebread's name for this unit is biotite quartz diorite. The mineral phases present are plagioclase (An 31; 45-55%), potassium feldspar (10-15%), biotite (10-15%), hornblende (10-15%), quartz (2-3%), magnetite (2-3%), and trace amounts of sphene, chlorite, and epidote. Chemically, this monzodiorite is slightly higher in SiO_2 and Na_2O and lower in MgO and CaO than the porphyritic type (Table 3).

Diorite

Diorite comprises about 1% of the rocks in the district and occurs as small irregular masses in the southern part of the district that are intruded by pegmatite and aplite dikes. Contacts with the monzodiorite gneiss are obscured by granitic dikes. The diorite is black to green, medium-grained (1-3mm), equigranular, and characteristically weathers to a reddish-brown irregular surface.

The diorite is hypidiomorphic-granular. The mineral phases present are plagioclase (45-50%), hornblende (10-30%), biotite (5-10%), and iron oxides. Secondary chlorite and sericite were observed. Subhedral to euhedral plagioclase crystals have a composition of An 44 (Andesine) to An 50 (Labradorite) and are typically mildly sericitized. Chlorite occurs as radiating masses around biotite or hornblende cores and as a very fine-grained material interstitial to the plagioclase.

Analyses indicate that the diorite is chemically a gabbro (Fig. 2). It contains much less SiO_2 and more Fe_2O_3 , MgO , and CaO than an average diorite (Table 3). The discrepancy is the result of Streickesen's division between a gabbro and diorite, which is based on plagioclase composition (diorite is defined as having $\text{An} < 50$ and gabbro as having $\text{An} > 50$), the plagioclase composition of this diorite is An 44-50.

Syenite

Pink, medium-grained (2-5mm) syenite intrudes the monzodiorite gneiss as small masses in the southeastern part of the district and comprises less than 1% of the district. This rock unit characteristically weathers to a brown, kaolinitic, limonite-stained, crumbly mass and is composed of orthoclase (65-70%), secondary quartz (25-30%), with traces of limonite, hematite, sericite, and apatite.

The syenites are hypidiomorphic-granular. Subhedral orthoclase are typically carlsbad twinned and contain hematite stain along the grain boundaries. Anhedral quartz occurs interstitial to the feldspar. It is finer-grained along grain boundaries and coarsens toward grain interstices, which suggests silicification.

Granite

Pink, fine to medium grained, equigranular granite comprises 4% of the district and occurs as irregular bodies and dikes that intrude all of the other Precambrian rocks in the district. Aplite and pegmatite dikes vary in width to a maximum of 6 meters. The granite characteristically weathers to a pinkish brown to white color. The granites are allotriomorphic-granular and are composed of microcline (35-50%), quartz (28-32%), plagioclase (10-25%), biotite (2-3%), with trace amounts of apatite, zircon, and iron oxides. The pegmatites commonly contain 1-2cm books of muscovite. A published U/Pb age from zircon for this unit is 1445 +/- 10 m.y. (Hedlund and Stacey, 1983).

The chemistry of this granite is higher in SiO_2 and K_2O and lower in MgO than an average granite (Table 3). These granites have similiar chemistry to A-type granites (Bowden, 1985).

Diabase and basalt porphyry

Northwest-trending, dark-gray to black, fine-grained (<1mm) diabase dikes occur in the southern half of the Black Hawk district. These dikes are up to six meters wide and comprise less than 1% of the rocks in the district. They characteristically weather to a greenish-gray smooth surface rock and intrude all of the Precambrian rocks.

The diabase is sub-ophitic and is composed of plagioclase(55-60%), pyroxene(25-30%), iron oxides(5-10%), and trace amounts of sericite and chlorite. The plagioclase laths(.3-.5mm in length) are albite twinned. Anhedral augite is interstitial to the plagioclase. Some of the pyroxene may be pigeonite as indicated by the low 2V.

Gillerman and Whitebread (1956) describe basalt porphyry dikes which are compositionally similar to the diabase but contain 0.5 cm feldspar phenocrysts (10-15%). These were not observed.

CRETACEOUS-TERTIARY LITHOLOGIES

Rhyolite

East-west trending, white rhyolite dikes occur in the district 30 meters south of the Black Hawk mine. They intrude all Precambrian rocks, are faulted, and are intruded by diorite porphyry dikes. They weather to a

limonite-spotted rock. They are altered and cut by quartz veinlets. In thin section, they are allotriomorphic-granular and are composed of quartz (60-70%), potassium feldspar (10-15%), limonite (biotite pseudomorphs; 1%), and sericite (20-30%). These rhyolites are approximately 5% higher in SiO₂ than an average rhyolite, which most likely is related to the quartz-sericite alteration (Table 3).

Diorite porphyry

The Twin Peaks diorite-porphyry stock, which intrudes the Precambrian porphyritic monzodiorite gneiss, is approximately five kilometers long and two kilometers wide; and is the second most abundant rock in the district. This unit also occurs as northeast-trending dikes and small masses in the southern and eastern parts of the district. The diorite porphyry is steel-gray, fine-grained, characteristically weathers to a white to greenish-gray resistant rock and is composed of an aphanitic groundmass (65-75%), with phenocrysts of plagioclase (20-30%), hornblende (3-6%), sanidine (1-2%), and minor iron oxides.

Subhedral plagioclase (An 32-36) phenocrysts are as large as 5mm but typically 1-2mm in size (up to 5mm), have albite twinning, and are normally zoned. They are mildly sericitized. A few sanidine phenocrysts have been observed which can be identified by their low 2V and Carlsbad

twinning. Subhedral to euhedral prismatic hornblende phenocrysts are generally 3-4mm, have green pleochroism and commonly alter to chlorite. Quartz is rare. The aphanitic matrix, which surrounds the phenocrysts contains minor amounts of carbonate veinlets. Hornblende from the Twin Peaks diorite-porphyry yielded a K-Ar age of 72.5 +/- 4.7 m.y. (Hedlund, 1980).

When compared to an average diorite and granodiorite, the Twin Peaks diorite porphyry is higher in SiO₂ and lower in TiO₂, Fe₂O₃, MgO, and CaO compared to an average diorite. It is similar to an average granodiorite except for higher Al₂O₃ and CaO values. Two diorite porphyry samples have slightly higher Co and slightly lower Ni values compared to an average intermediate igneous rock (Fig. 4).

Granodiorite

Granodiorite dikes occur in the northern part of the district. Gillerman and Whitebread's name for this unit is quartz diorite. The granodiorite is light to medium-gray, fine-grained, equigranular, and consists of plagioclase (50-55%), quartz (15-22%), alkali feldspar (10-12%), hornblende (4-11%), and minor amounts of chlorite, sericite, and iron oxides. Epidote veinlets occur in some of the samples. These dikes cut the diorite-porphyry dikes and are commonly less than five meters wide.

Andesite

Blue-gray andesites occur as two small oval-shaped masses northeast of the Black Hawk mine and intrude the monzodiorite gneiss and granite. The masses have columnar jointing along their contact with the gneiss. They are composed of a cryptocrystalline groundmass (65-70%), which is commonly carbonatized and sericitized. Phenocrysts consist of plagioclase (8-20%) and hornblende (1-3%), and minor amounts of biotite and chlorite.

Beartooth quartzite

North-dipping Beartooth quartzite unconformably overlies the Precambrian rocks in the northern part of the district. Colorado shales lie conformably above the Beartooth quartzite seen outside the district. This quartzite is a white, fine grained (<1mm), well sorted, and well rounded quartz arenite. Crossbedding occurs near the base of the formation. A pebbly chert conglomerate is found at the base of this unit that is cemented by quartz and is intertongued with laminations of shale.

QUARTERNARY LITHOLOGIES

Alluvium occurs in the Black Hawk Canyon. It is composed of sand, gravels, and boulders of the surrounding rocks.

Faults and Fractures

Structural features are shown on Plate 1. The oldest set of fractures are northwest-trending. They generally strike N 45-65° W and dip to the southwest. Diabase dikes occur along some of these structures. These fractures cut the older Precambrian rocks and are then cut by younger, diorite-porphry dikes and northeast-trending faults.

There are two major fault systems in the Black Hawk district. Each system consists of one major, northeast-trending structure with several steeply-dipping faults that splay off to the northeast. One of these major faults passes through the middle of the district from north to south approximately 100 meters west of the Black Hawk mine. The other major system occurs several hundred meters east of the Black Hawk mine. Silver mineralization occurs in the northeast-trending faults, which branch from the major structures. There are also northeast-trending shear zones that occur within the Twin Peaks stock and along the stock's contact with the porphyritic monzodiorite gneiss. These northeast-trending structures cut all the rocks in the district except for the small, neck-shaped, andesite intrusions (Kan) in the northeastern portion of the study area.

Post-ore faulting is common. An example of this faulting was seen in the 8th level of the Black Hawk mine (Gillerman and Whitebread, 1956). This fault strikes N 75° E, dips 25 to 30° NW, and displaces the ore below the 8th level.

Mineralization

All silver mineralization is found in ankerite-bearing veins, which generally follow the major northeast-trending faults and fracture systems. There are approximately four kilometers of identified veins with about 5% of these structures containing known silver mineralization (Gillerman and Whitebread, 1956). The veins are hosted principally by the porphyritic monzodiorite gneiss.

The Black Hawk vein has a strike length of 600 meters and dips 70-75 degrees to the northwest. Ore occurs in dilatant zones and is commonly surrounded by greatly fractured porphyritic monzodiorite gneiss and a precursor sulphide stage. This sulphide stage consists of pyrite and pyrrhotite that occurs as disseminated grains and veinlets in the porphyritic monzodiorite (Fig. 5). It also occurs as replacements of mafic minerals in the Twin Peaks diorite porphyry. Near the vein, pyrite has undergone various degrees of brecciation and replacement. Pyrite is typically replaced by chalcopyrite and sphalerite. Pyrrhotite occurs as rounded blebs surrounded by pyrite. This sulphide stage

is common in the porphyritic monzodiorite gneiss, but it is very rare in the carbonate veins. Average vein width is about 0.5 meters but may open into swells of up to 3 meters. High-grade ore pockets range in size from 1cm. in width to shoots extending 20 meters vertically, 10 meters horizontally, and 1 meter wide (Gillerman, 1964).

The ankerite-bearing veins are fine-grained, white to pink in color when fresh and chocolate-brown when weathered (Fig. 6). Brecciation of the vein is common. The term ankerite is used in this study for the carbonate veins since Von Barga (1979) determined an anomalous amount of Fe and Mg to be present in the carbonate. Quartz is cryptocrystalline typically surrounding wallrock-fragments within these veins. Barite is only present in minor quantities. Significant ore minerals at the Black Hawk district are native silver, argentite, niccolite, rammelsbergite, nickel skutterudite, galena, sphalerite, chalcopyrite, and uraninite.

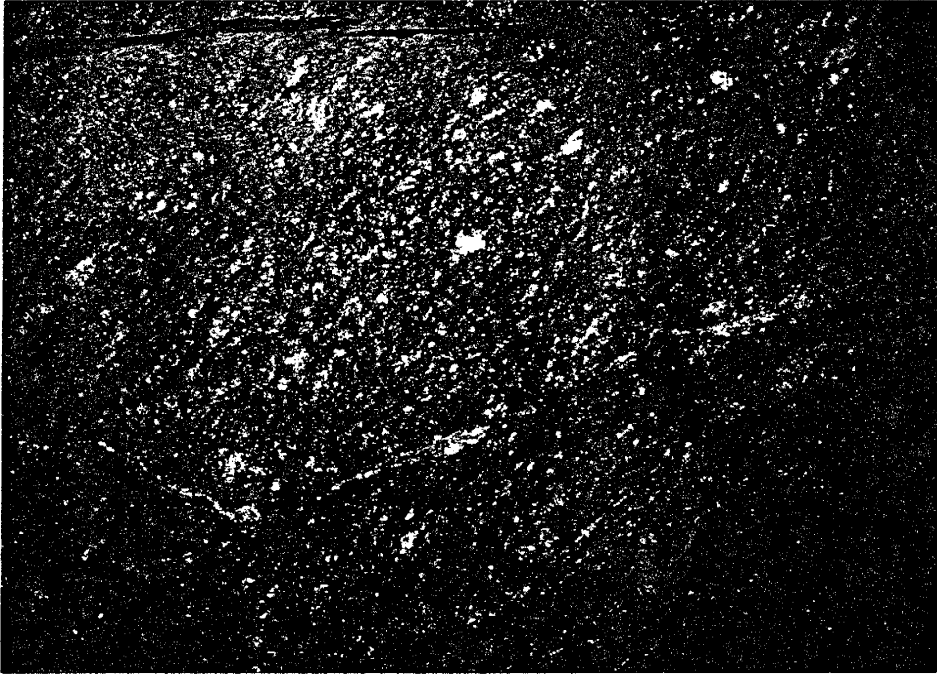


Figure 5. Photograph of the porphyritic monzodiorite showing the precursor sulphide stage of pyrite.

1977

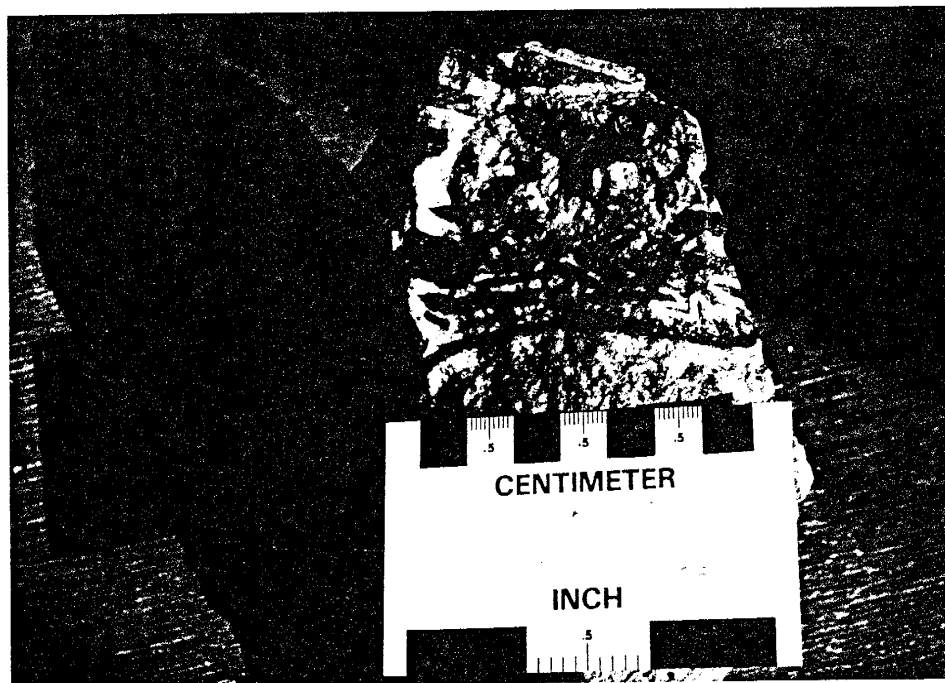


Figure 6. Photograph of a hand sample of weathered ankerite vein. Notice the chocolate-brown color from weathering. Black clasts are altered country rock.

Alteration Assemblages

Two distinct aerial patterns of alteration have been recognized within the rocks exposed at the Black Hawk deposit (Plate 1) on the basis of field mapping supported by thin section studies. Areas that are mapped as unaltered, however, may be slightly altered when observed in thin section. First, there is a fairly widespread alteration which is apparently associated with the unconformity between the Precambrian porphyritic monzodiorite gneiss and the upper Cretaceous Beartooth quartzite. And secondly, there are two types of vein-related alteration; these are intermediate argillic and propylitic alteration assemblages, which are the systems of interest in this study. Intermediate argillic and propylitic alteration assemblages crosscut all rock types principally along the northeast-trending faults and shear zones. The precursor sulphide stage is spatially associated with these alteration assemblages. Both of the vein-related alteration assemblages were present when mineralization was observed, but mineralization was not always present when the alteration assemblages were observed. Therefore, no distinction can be made between barren and ore zones on the basis of the associated alteration. Since the vein-related alteration affected the Twin Peaks intrusive then this suggests that alteration formed during the late stages or after cooling of the intrusive. The geometry and intensity

of the vein-related alteration types are strongly affected by fracture density and fracture distribution in wall rocks adjacent to the vein. An idealized sketch of the horizontal zoning of the vein-related mineralogical and textural alterations is shown in Figure 7 . The lack of an adequate vertical control prohibited this study from testing vertical alteration zonations. The mineralogy of the alteration assemblages is discussed below.

The widespread alteration associated with the Beartooth unconformity is 30 to 40 meters thick and occurs in the northern half of the Black Hawk district (Plate 1). Similar alteration is seen along the Beartooth unconformity in the Saddle Rock Canyon, northwest of the study area. This alteration type is best observed in the porphyritic monzodiorite gneiss and is recognized in the field by the distinct mottled, yellowish-brown and white color, limonite staining, and crumbly rock (Fig. 8). The mineral assemblage in this zone is principally clay, limonite, chlorite, and relict crystals of plagioclase, orthoclase, biotite, and quartz. The regional nature of this alteration and occurrence under a sedimentary unit suggests that it is a paleo-regolith.

Intermediate argillic alteration assemblages occurs along most of the veins (Plate 1 and Fig. 7) and is recognized in the field by the abundance of white clay

Figure 7. Idealized diagram of the textural and mineralogical relations of the alteration at the Black Hawk mine. No scale is given.

MINERALOGICAL ALTERATION

TEXTURAL ALTERATION



VEIN

QUARTZ

CLAY

SERICITE

PYRITE

ANKERITE

CHLORITE

LEUCOXENE

MAGNETITE

EPIDOTE

no relict crystals

relict feldspar
crystals preserved

relict feldspar and
mafic crystals
preserved

original texture
preserved

and sericite (Fig. 9a).

Areas of intermediate argillic alteration and the regionally altered rocks are indistinguishable where they occur together. The contacts between intermediate argillic alteration and propylitic alteration are usually gradational but may be sharp (Fig. 9d). In thin section, the feldspars are completely replaced by clay, sericite, carbonate, and quartz and mafic minerals are replaced by sericite, pyrite, and other iron oxides (Fig. 9b and 9c). The amount of clay, carbonate, and quartz is most abundant near the vein and decreases towards the propylitic alteration.

Propylitic alteration grades out from the intermediate argillic alteration towards unaltered rocks (Fig 7) and is recognized in the field on the basis of pale to dark green color (Fig. 9d), abundance of visible chlorite in the porphyritic monzodiorite gneiss, and a purplish-red color in the diorite porphyry. In thin section of porphyritic monzodiorite gneiss, the hornblende and biotite are replaced by an intergrowth of chlorite and magnetite (Fig. 9e). Some hornblende is partially replaced by epidote. Plagioclase in these rocks is altered to sericite (Fig. 9e) and less commonly to carbonate. Alkali feldspars are commonly unaltered to slightly sericitized. Relict crystals can be recognized in this zone.

(37)

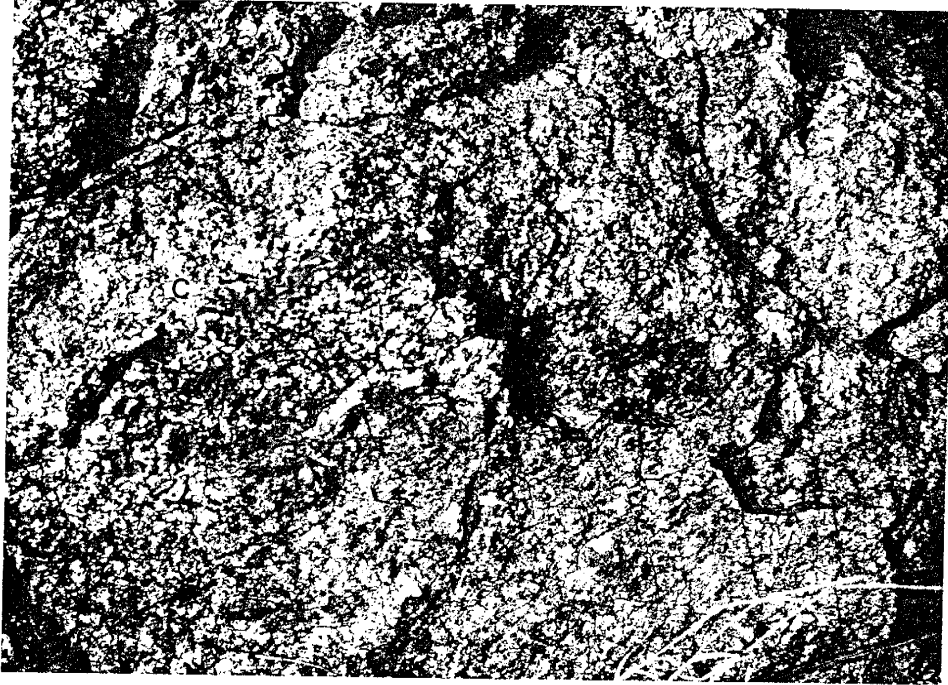
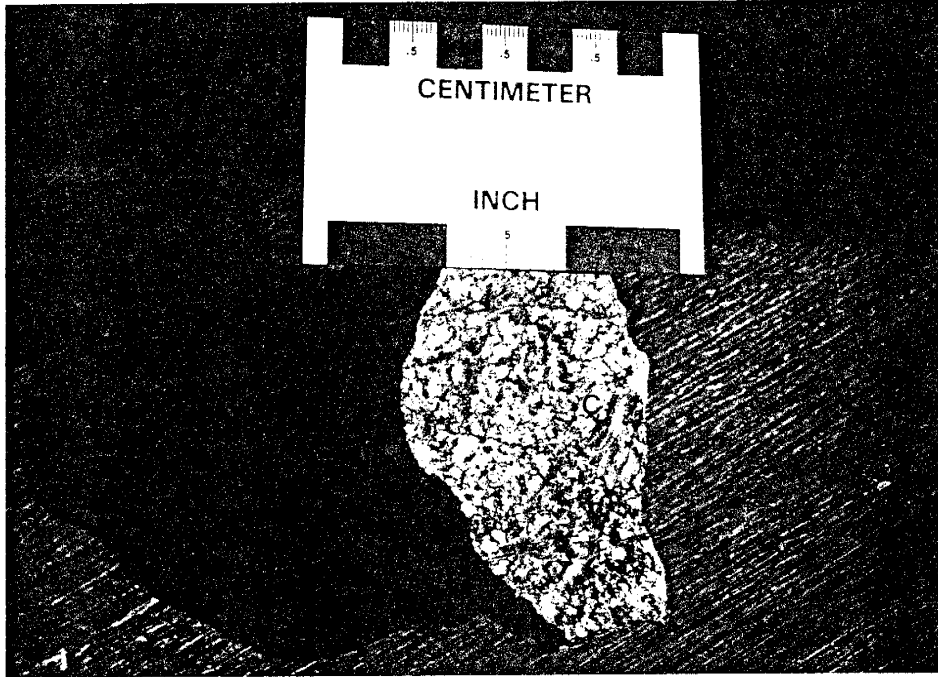
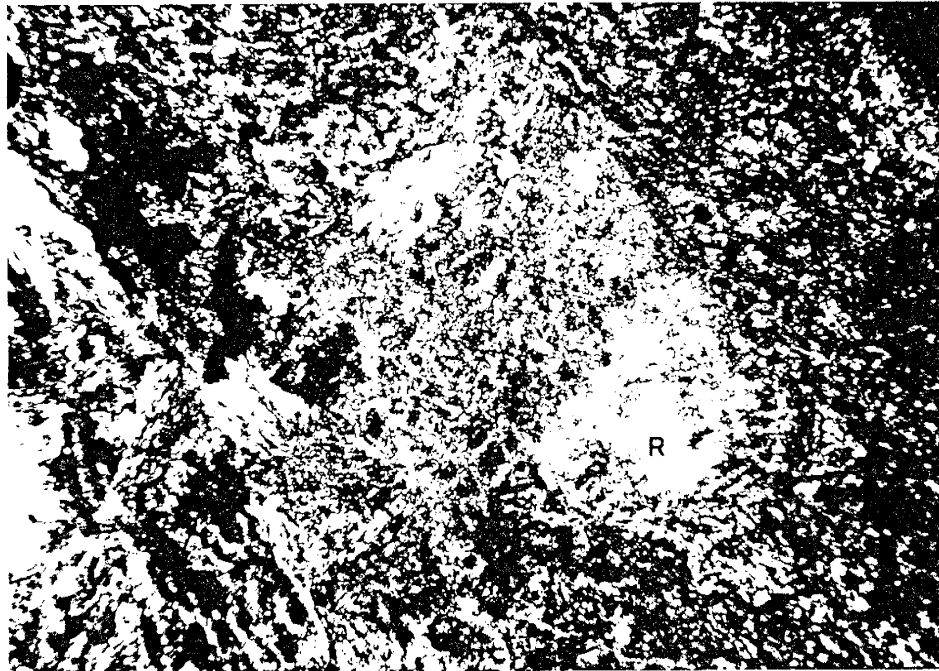


Figure 8. Photograph of an outcrop of the inferred paleo-regolith at the Cretaceous-Precambrian unconformity. Original feldspars are altered to clay (C) with some of the original crystals preserved (P). Biotite is altered to limonite (L) and chlorite.

Figure 9. Alteration assemblages in the porphyritic monzodiorite gneiss. a) Hand specimen of intermediate argillic alteration. Characterized in the field by white clay(C) and sericite(S). b) Photomicrograph of intermediate argillic alteration showing relict crystals(R). c) Photomicrograph of intermediate argillic alteration showing relict crystals destroyed. d) Hand specimen showing the contact between intermediate argillic and propylitic alteration assemblages. e) Photomicrograph of propylitic alteration showing replacement of feldspars by sericite(S) and replacement of biotite by an intergrowth of magnetite and chlorite(C). f) Hand specimen of unaltered gneiss. g) Photomicrograph of unaltered gneiss.



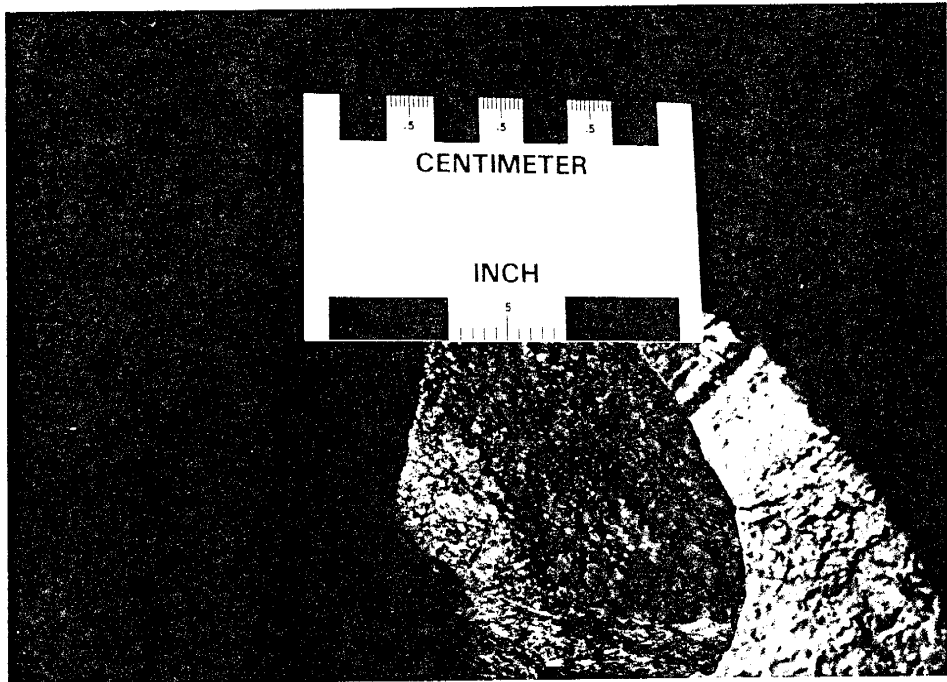
A



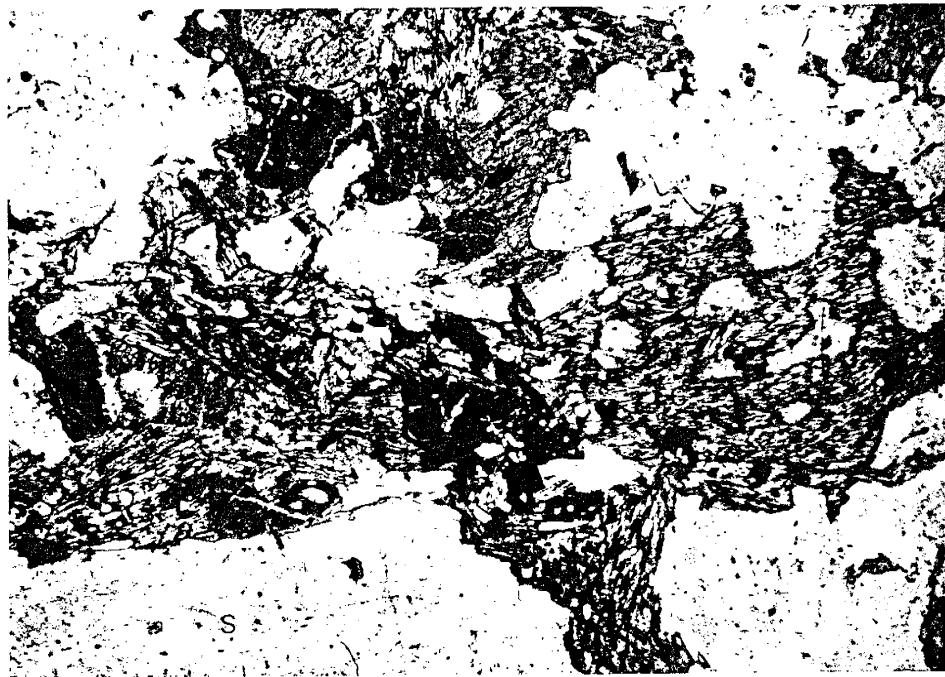
B



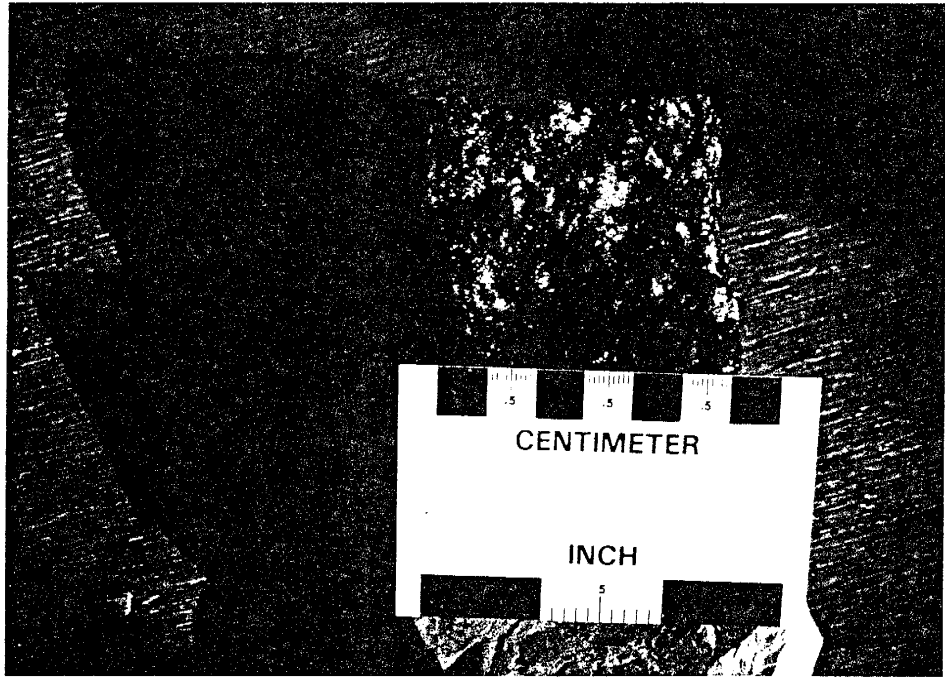
C



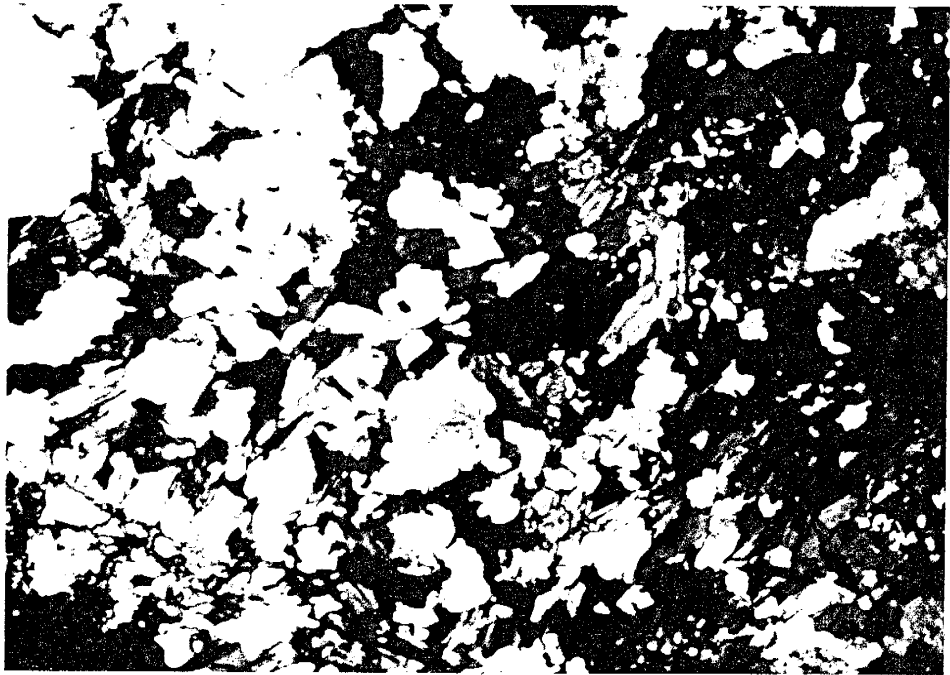
D



E



F



G

For comparison, photographs of unaltered, porphyritic-monzoiorite gneiss are shown in Figures 9f and 9g. Plagioclase crystals may be slightly sericitized (Fig. 9g). This rock type consists dominantly of plagioclase, biotite, and hornblende with minor amounts of quartz, alkali feldspar, and magnetite.

Geochemistry of the Hydrothermally Altered Monzoiorite

XRF analyses of fresh, propylitized, and intermediate argillized porphyritic-monzoiorite gneiss are presented in Appendix A. These analyses have been recalculated to 100% and then the altered analyses have been recalculated on the basis that alumina has remained constant during alteration (Krauskopf, 1979, p.82-83). The analyses indicates that the propylitic alteration process resulted in the addition of H_2O , K_2O , and Na_2O to the rocks and depletion in CaO , MnO , and total Fe and the intermediate argillic process resulted in the addition of H_2O , SiO_2 , total Fe, MnO , MgO , and CaO and depletion in K_2O , Na_2O , and TiO_2 (Table 4).

Table 4. Recalculated analyses of porphyritic monzodiorite gneiss

	Unaltered 113-6B	Propylitic	Intermediate argillic
SiO ₂	55.00	57.88	59.93
TiO ₂	1.50	1.52	1.37
Al ₂ O ₃	18.12	18.12	18.12
Fe ₂ O ₃	9.22	8.21	10.06
MnO	.16	.10	.46
MgO	2.59	3.70	3.45
CaO	5.48	2.27	7.91
Na ₂ O	4.09	4.93	.33
K ₂ O	2.63	3.71	2.40
P ₂ O ₅	.40	.38	.39
LOI	.81	3.54	14.55
TOTAL	100.00	104.36	118.55

Fluid Inclusion Study

Fluid inclusions from twenty-five quartz, ankerite, and sphalerite doubly-polished sections were examined. Because of the fine-grained nature of the mineral, few inclusions were found for microthermometry measurements. Fluid inclusions from seven samples from the Black Hawk mine and three samples from the Alhambra mine could be measured. Visual uncertainty, calibration errors, and reproducibility limited the accuracy of Th measurements to ± 10 °C and errors of up to 1 eq.wt.% NaCl in salinity determinations. Fluid inclusion data and general sample locations are given in Appendix C.

Four types of inclusions are recognized (Fig. 10). Type I is a one-phase, liquid-only inclusion. This type is found in all the samples and is most abundant along fractures. Type II has liquid and a vapor bubble that occupies less than 50 volume percent of the inclusion and is the most common type of inclusion found. Type III contain liquid and a vapor bubble that occupies greater than 50 volume percent of the inclusion and homogenize to vapor. Type IV has vapor, liquid, plus a solid identified as halite. The size of the inclusions range from less than 1 to 25 microns in their longest dimension and the average size for measurable inclusions is 10 microns. Only inclusions with no planar arrangement were measured; these are interpreted to be primary inclusions (Roedder, 1984).

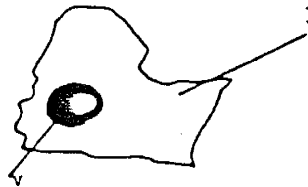
Fluid inclusions of the pre-ore stage were studied in quartz from samples of altered wall rock in the Black Hawk mine where pyrite occurs intergrown with the quartz. Type II and III fluid inclusions were numerous and characterize the pre-ore stage. The only identified daughter mineral present was halite. A wide range of Th were measured, 290 to 410 °C, with a low salinity of about 2 eq.wt.% NaCl, except for a few Type IV inclusions which had a salinity of about 40 eq.wt.% NaCl.

Figure 10. Representative sketches of the four types of fluid inclusions observed (l, liquid; v, vapor; h, solid).

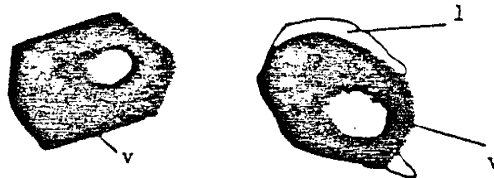
TYPE I:



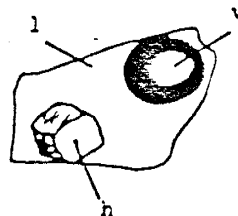
TYPE II:



TYPE III:



TYPE IV:



Numerous Type II and III fluid inclusions coexist at temperatures greater than 360 °C. This suggests boiling during mineral deposition. Inclusions above 375 °C exhibit supercritical fluid behavior. This is recognized by the abrupt and complete fading of the meniscus between liquid and vapor (Roedder, 1985).

Type II inclusions characterize the main-ore stage (Von Barga's arsenide Stage) which have native silver, niccolite, rammelsbergite, and ankerite intergrown. Vapor-rich inclusions were observed with liquid-rich inclusions in this stage. It was possible to measure Th on only 3 of these. Type II inclusions, which are the most common, exhibit Th of 160 °C to 290 °C, with an average of 220 °C. Calculated salinities are typically less than 4 eq.wt.% NaCl.

Type II fluid inclusions are the only type of inclusion in sphalerite from the late stage (Von Barga's sulphide stage). Average Th for this stage is 190 °C, ranging from 160 °C to 220 °C and a calculated salinity of 1 eq.wt.% NaCl. Homogenization temperatures (Th) and salinities are shown in histogram form (Figs. 11 and 12) grouped according to their stage of mineralization.

Figure 11. Frequency histograms of T_h of fluid inclusions. Unfilled areas in histograms represents Type II inclusions and filled areas are Type III inclusions.

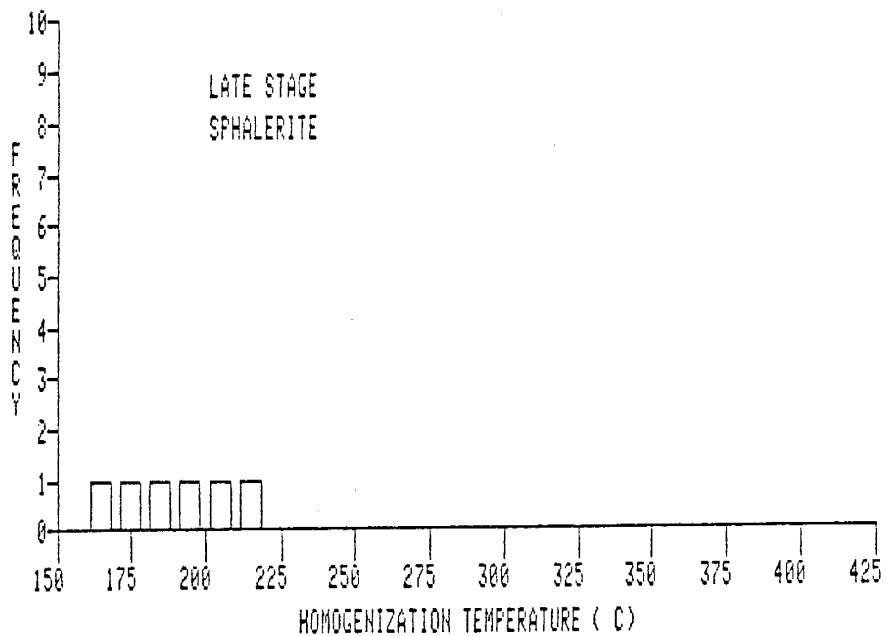
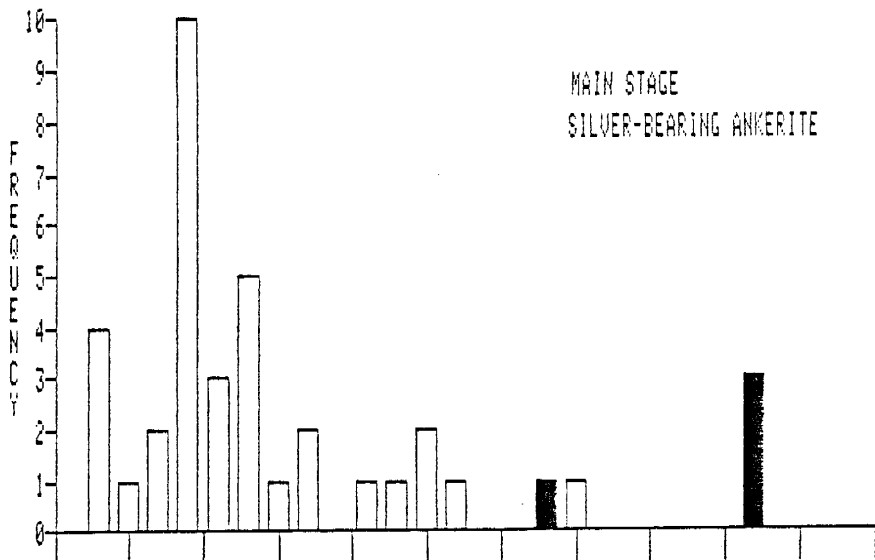
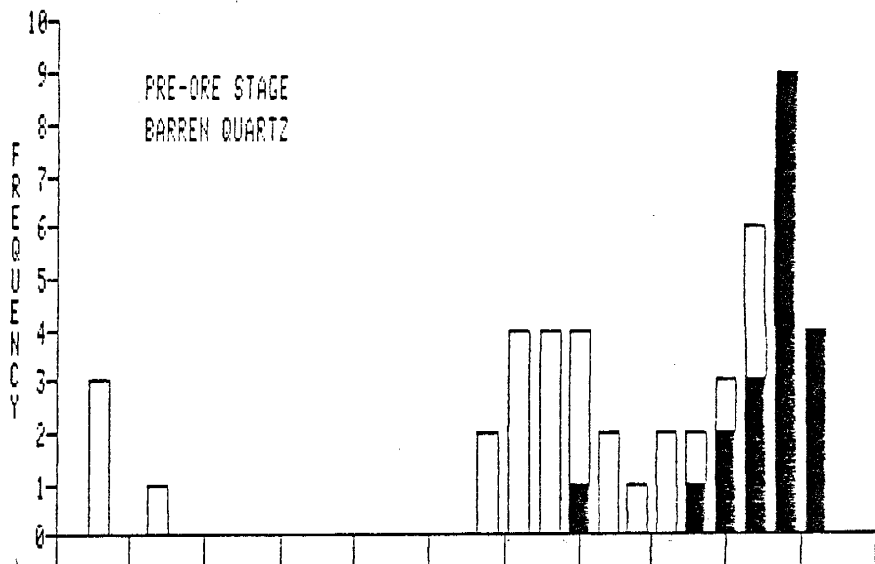
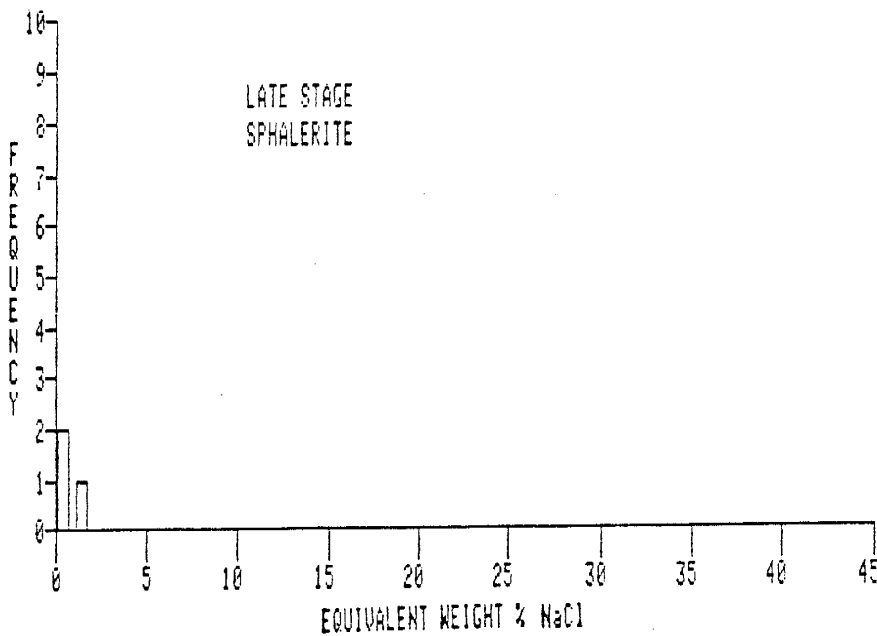
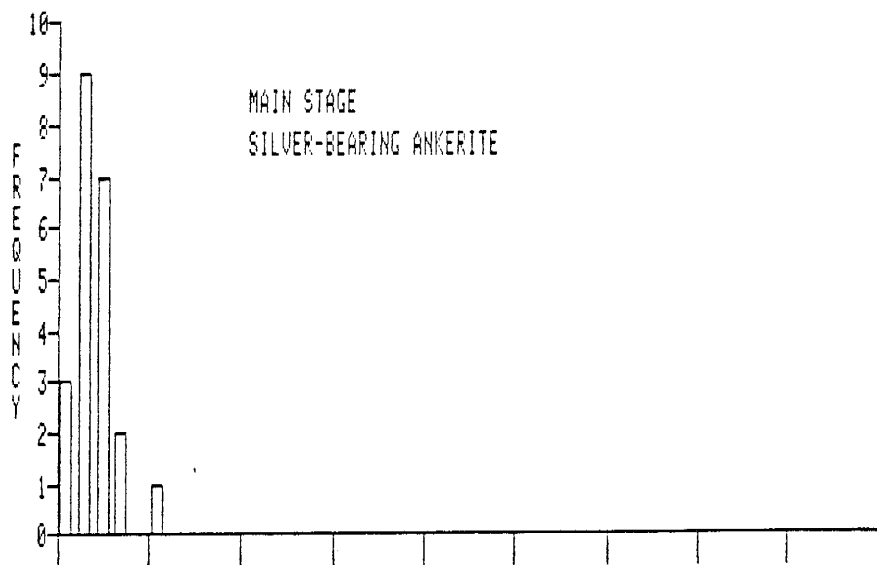
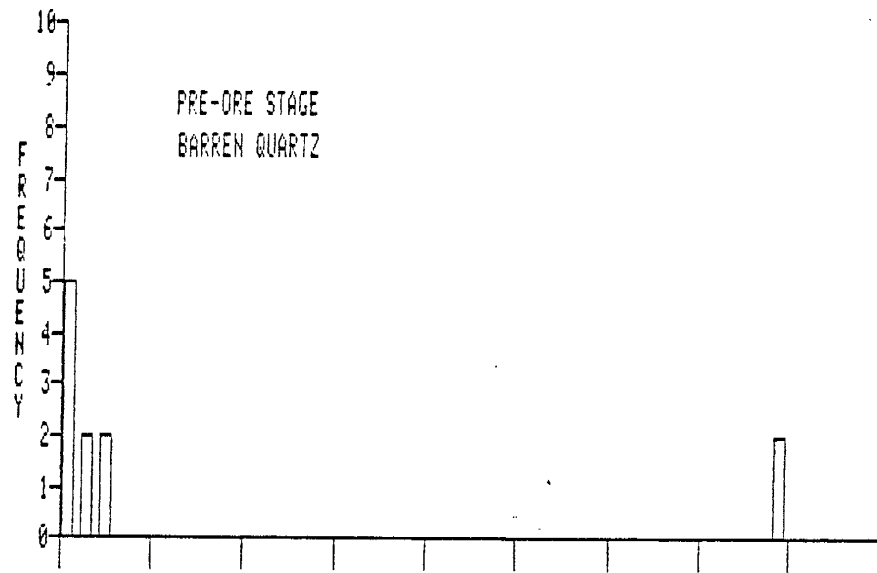


Figure 12. Frequency histograms of calculated salinities of fluid inclusions.



K-Ar Dates

Two samples were analyzed by K-Ar dating methods (Table 5):

Table 5. K-Ar dates from the Black Hawk District

Rock type	K (wt.%)	40Ar (mol/gmx10(11))	40Ar (% of total 40Ar)	Age (my)
Porphyritic monzodiorite gneiss	1.92	299.9	98.75	703 +/-32
		272.7	96.86	
		Av. 286.3		
Intermed. arg. vein alter.	1.516	17.69	74.77	65.3 +/-1.2
		17.28	71.57	
		Av. 17.49		

Note: Analyses were determined by Anne Wright; uncertainties are at the 68% confidence level.

They are a whole-rock sample of the intermediate argillic alteration associated with the veins and a biotite/hornblende split from the porphyritic monzodiorite gneiss. Since the intermediate argillic alteration appears to be contemporaneous with the mineralization, the date of the alteration should date the mineralization. The validity and interpretations of these dates are discussed in a later section.

DISCUSSION

Pressure and Depth of Mineralization

Fluid inclusion data suggests that two types of fluids produced the mineralization at the Black Hawk district; these fluids are a low salinity (< 2 eq.wt.% NaCl), supercritical fluid for the pre-ore stage and a low salinity (< 5 eq.wt.% NaCl), nonboiling fluid for the main ore stage. It is unclear from this study whether the fluids were from one magmatic solution which evolved during cooling or from fluids of different origin.

The presence of two high salinity (40 eq.wt.% NaCl) fluid inclusions with NaCl poor vapor-rich inclusions may represent the unmixing of a supercritical fluid. According to Sourirajan and Kennedy's data (1962), the unmixing of a 400 °C critical NaCl-H₂O (2.6 wt% NaCl, 285 bars) fluid can produce a very saline liquid (~40wt.% NaCl) and a coexisting NaCl poor vapor phase (~.01 wt% NaCl).

A pressure estimate of mineral deposition is possible from the fluid inclusion data where boiling is indicated. The majority of boiling is indicated in the pre-ore stage at 380 °C from a 2 eq.wt.% NaCl solution. At this temperature, the estimated minimum pressure is 270 bars, assuming a NaCl-H₂O system (Sourirajan and Kennedy, 1962). If this pressure is hydrostatic, it corresponds to a depth of about 2.5 kms. (Haas, 1971); if lithostatic pressure existed,

the indicated depth of mineral formation is about 800 meters, assuming a rock density of 2.84. Since repeated brecciation and cementation of the veins suggests opening and sealing of the fractures, both hydrostatic and lithostatic pressures probably existed during ore formation. If other gases such as CO₂ existed in the fluids then the pressure may be even higher. Von Barga (1979) estimated the depth from the paleosurface to the Black Hawk collar to be approximately 671 meters from geologic considerations with a maximum and minimum of 1372 and 274 meters respectively when mineralization occurred. These values are consistent with the depth estimates by fluid inclusion geobarometry.

Fluid inclusions from the main stage have lower homogenization temperatures than the pre-ore stage except for five inclusions. These five inclusions may represent remnant fluids from the earlier stage. Since this main stage was dominated by nonboiling fluids, a pressure and depth estimate may not be made. A minimum temperature correction of +15 °C can be estimated if a pressure of 270 bars and a salinity of 2 eq.wt.% NaCl is assumed. This yields an average temperature of 235 °C for the main stage of mineralization.

Mechanism for Mineral Deposition

It can be speculated from the geochemistry data that the source for the ore and gangue elements was the surrounding country rocks. Depletions of several major elements such as Ca, Mg, and Fe occur within the propylitized rocks and the enrichment of these elements in the ore zone indicate that the fluid was leaching these elements and depositing them in the structures. Silver and base metals were probably transported in solution as chloride complexes (Barnes, 1979) and uranium as CO_3 complexes (Rich et al., 1977). Little is known about the transportation of nickel and cobalt (Barnes, 1979).

The mechanism for mineral deposition must explain the association of carbonate gangue minerals, native silver, Ni and Co arsenides, and uranium as the main stage and the abundance of base metal sulphides as a late stage in the paragenetic sequence. Since carbonate minerals have an inverse solubility with temperature, their deposition is principally in response to increases in pH, which can result from wallrock reactions (Barnes, 1979). The alteration assemblages observed at the Black Hawk district explains this increase in pH of the solution as a result of hydrolysis of the feldspars and mafic minerals to form micas and clays, which are common H-ion consuming reactions. Experimental data suggests that silver and carbonate mineral

deposition are favored at a pH > 4 (Barnes, 1979). Little is known about the solubility of Ni and Co arsenides but Naumov et al. (1971) suggests that the veins rich in arsenides may result from hydrothermal fluids with low sulfur concentrations that react with the wallrocks. The total replacement of pre-ore pyrite by base metals suggests that the solution was low in sulfur and deposition resulted from the addition of sulfur ions from the pyrite in the wallrocks. Rich et al. (1977) examined the solubility of uranium and indicate that deposition of uranium may result from reduction by solution /wallrock reactions. Therefore, the alteration assemblages, ore and gangue minerals suggests that the main mechanism for Ag-Ni-Co-As-U deposition was solution /wallrock reactions principally resulting in the increase of the pH and sulfur concentration of the ore solution. A decrease in fluid inclusion homogenization temperatures from the pre-ore stage through late stage mineralization suggests that cooling may have played a role in mineralization but to what degree is uncertain.

Age of Mineralization

The reliability of K-Ar dating methods for Precambrian rocks is questionable. Ar losses due to metamorphism, weathering, and mechanical means will result in an underestimate of the rock's age. There is a discrepancy of approximately 700 m.y. between the two reported dates for

the porphyritic monzodiorite gneiss (Table 6). The reason for this discrepancy is most likely due to the locations of the samples. The oldest date was a sample collected away from any intrusives, whereas, the youngest date came from a sample located next to the Twin Peaks intrusive so that contact metamorphism may have reset the date. Therefore, the best conclusion from these dates is that the porphyritic monzodiorite was at least Proterozoic.

Table 6. K-Ar date comparison of various rocks in the vicinity of the Black Hawk deposit

Rock type	Age	Reference
Porphyritic monzodiorite gneiss	1380+-45m.y. 703+-32m.y.	Hedlund, 1980 This study
Twin Peaks diorite porphyry	72.5+-4.7m.y.	Hedlund, 1980
Vein alteration	65.3+-1.2m.y.	This study
Tyrone quartz monzonite	56.2+-1.7m.y.	Hedlund, 1980

The Laramide age (Table 6) of both the vein alteration and the Twin Peaks and Tyrone intrusives as well as the close spatial relationship between the mineralization with the Twin Peaks stock suggests that the age of mineralization was Laramide. Since mineralized veins cut the Twin Peaks stock, then the age of mineralization is at least as young as the late stages of cooling of the stock. The younger age for the vein alteration from this study compared to

Hedlund's age for the Twin Peaks intrusion suggests that younger hydrothermal events may have partially reset the dates. However, if one assumes a lower confidence level for the dates then the two values are in agreement.

Comparison with Other
Ag-Ni-Co-As-U Type Deposits

Other occurrences of Ag-Ni-Co-As-U mineralization comparable to the Black Hawk district were summarized by Bastin (1935). Although there has been a limited amount of new data published on this type of deposit it is enlightening to compare the Black Hawk district with three of the best documented districts with comparable mineralogy.

GEOLOGIC SETTING

The geology for Kongsberg, Norway: Great Bear Lake, N.W.T.; and Cobalt-Gowganda, Ontario have been described by Gammon (1966); Robinson and Ohmoto (1973); and Jambor (1971), respectively. All are similar to the Black Hawk district in some way. All of these deposits occur within Precambrian batholithic complexes, which consists of metasediments and metavolcanics intruded by calc-alkaline intrusives. Unconformable, younger sediments consistently overlie this batholithic complex. More igneous activity followed with calc-alkaline intrusives. The composition of the intrusives ranges from granitic to diabasic. Within the

older rocks there is a precursor sulphide stage, which appears to be spatially associated with the younger, silver mineralization. The sulphides were formed as sediments, exhalatives, skarns, or from early hydrothermal activity. The age for silver mineralization is highly variable but is described as always being associated with late intrusive activity.

The geology of the Kongsberg, Norway deposit consists of Precambrian (1500m.y.) metavolcanics and metasediments of the Kongsberg-Bamble complex (Gammon, 1966). This formation consists of banded gneisses and dioritic gneisses, amphibolites, and granites and has occurrences of fahlbands, which are sulphide-rich units conformable to the rock lithologies and possibly of exhalative origin. In the Kongsberg region, fahlbands are up to 15 km long, with widths of 300 meters. Middle Cambrian conglomerates and black shales unconformably overly these Precambrian rocks. Igneous activity during a Permian rifting event is characterized by basic and granitic intrusives. Permian diabase dikes intrude the older rocks and are associated with quartz-sulphide veins. Silver-calcite mineralization occurs crosscutting the older quartz-sulphide veins. It has been suggested that the silver veins are associated with the intrusion of Permian granites (Segelstad, personal comm.).

Robinson and Ohmoto (1973) describe the geology of the Great Bear Lake Region as consisting of the Great Bear Batholithic Complex, which is comprised of middle Proterozoic, calc-alkaline volcanics, coeval sub-volcanic porphyries, and associated sedimentary rocks, unconformably overlain by conglomerates, graywackes, and arkoses that were intruded by granite. These are overlain by more volcanic and sedimentary rocks. Sulphide-skarn mineralization is associated with the granites. This is followed by the intrusion of 1400 m.y. old quartz diabase dikes, which appear to be genetically related to silver mineralization.

The geology of the Cobalt-Gowganda area, as described by Jambor (1971) consists of Archean, Keewatin rocks which are predominantly fine-grained, intermediate to mafic volcanics interbedded with cherts and pyroclastics. Intrusions of quartz-feldspar porphyries also occur. This series of rocks is metamorphosed to greenschist facies. Sulphide bands occur within these rocks. Batholithic granites intrude these metavolcanics and metasediments at 2.5 b.y.. Unconformably overlying the Keewatin series are Proterozoic, Huronian rocks which consists of conglomerates, greywackes, quartzites, and arkoses. Disseminated sulphides occur at the base of the Huronian sediments and decrease upward. Silver mineralization occurs associated with the sulphide-rich sediments. Nippising diabase, which is a complex sill-like intrusion, intrudes all the previously

mentioned rocks. Silver mineralization occurs restricted to this diabase and is believed to be related to it.

GEOCHEMISTRY

A brief comparison of the physical and chemical environment at the time of mineralization for several Ag-Ni-Co-As-U type deposits is presented based on fluid inclusion and other data.

Table 7. Inferred physicochemical parameters for hydrothermal fluids for several Ag-Ni-Co-As-U deposits

Parameter	Kongsberg	Great Bear Lake Area	Cobalt-Gowganda Area	Black Hawk District
Temp. (°C)	190-300 (260)	95-200 (200)	100-560 (230)	160-410 (230)
Estimated pressure (bars)	150	280-500	600	270
Depth (km)	1.0	2.5-4.5	1-2	2.5
Salinity (eq.wt.%NaCl)	0-10	up to 30	up to 54	0-6
Evidence of Boiling	yes	yes	yes	yes
pH	6-8	4.0		4-6

() indicates the inferred temperature for silver mineralization. Data are from Kongsberg (Segelstad, personal comm.); Great Bear Lake (Robinson and Ohmoto, 1973); and Cobalt-Gowganda (Scott and O'Connor, 1971; Strong et al., 1984).

From this comparison, it can be seen that a large variation in temperatures occurred. However, silver is noted to have precipitated at about 230 °C in all deposits. Salinities are variable but most of the deposits have some high

salinity inclusions. The estimated depth at the time of mineralization for these deposits is generally less than 2.5 kilometers. However, the estimated depth for mineralization of the Great Bear Lake area is possible as high as 4.5 km.

MINERALIZATION

The mineralogy for Ag-Ni-Co-As-U type deposits is complex but consistent. In general the sequence is as follows : U + Quartz; followed by Ag + (Ni,Co,Fe) Arsenides + Dolomite; and finally Bi + (Cu,Pb,Zn) Sulphides + Sulphosalts (Badham, 1975). Gold is rare. Brecciation of the veins is common suggesting that repeated movement along fractures allowed for multiple events of opening and sealing of the vein. Badham (1975) indicates that the variations in paragenesis seen from deposit to deposit may be caused by differences in timing when the veins become open to ore-fluids. The differing abundance of individual mineral phases from deposit to deposit may reflect amounts of elements in the ore solution as well.

Similarities in mineralization and paragenesis are obvious when paragenetic diagrams are compared (Figs. 13 and 14). Initial mineralization at the Great Bear Lake area and the Black Hawk district consists of an early hematite and quartz phase. In addition to these minerals, Von Bargen (1979) describes the presence of pyrite and pyrrhotite as well in the Black Hawk district. The arsenide stage at the

Figure 13. Paragenetic sequence of the Echo Bay vein, Great Bear Lake area (Robinson and Ohmoto, 1973). Points A to G represent characteristic mineral phase (or phases): A, hematite; B, first appearance of dolomite; C, first appearance of native silver; D, first appearance of acanthite (argentite); E, appearance of marcasite; F, first appearance of the mineral assemblage, acanthite + chalcopyrite + carbonates; G, change from acanthite to native silver.

MINERALS \ STAGES	1	2	3	4	5	6	7
McKinstryite							—
Native bismuth			—				—
Native silver			—	D	F	G	
Acanthite			C				
Galena					—	—	
Sphalerite					—		—
Chalcopyrite					—	—	
Bornite					—		
Marcasite				E	F		
Calcite					—		
Dolomite			B		—		
Skutterudite							
Rammelsbergite			—				
Niccolite							
Pitchblende							
Quartz							—
Hematite	A						

Figure 14. Paragenetic sequence of the Black Hawk vein (Von Barga, 1979).

Mineral	Preore	Arsenide	Sulfide	Supergene
Silver		— —	—	
Niccolite		—		
Rammelsbergite		—		
Nickel				
Skutterudite		— —		
Gersdorffite		— —	—	
Argentite		— —	—	
Pyrite	—			—
Galena			— —	
Sphalerite			— —	
Chalcopyrite			— —	
Cubanite			—	
Bornite				—
Tennantite			— —	
Covellite				—
Digenite				—
Pearceite				—
McKinstryite				—
Jalpaite				—
Bravoite				—
Millerite			—	—
Siegenite			—	—
Bismuthinite				?
Molybdenite	?			
Pyrrhotite	—			
Uraninite		— —		
Manganite				—
Quartz	—		— —	
Kaolinite				—
Chlorite	—			—
Garnierite				—
Hematite	—		—	—
Goethite				—
Dolomite	—			
Siderite		— — —	—	
Calcite				—
Barite	—			—
Gypsum				—
Erythrite				—
Annabergite				—
Aurichalite				—
Azurite				—
Bismutite				—

Black Hawk is the equivalent of stages 2,3, and 4 for the Great Bear deposit. Native silver appears and is precipitated with (Ni, Co, Fe) arsenides. A consistent zoning of the arsenides is recognized. Niccolite is the first to appear followed by rammelsbergite, and finally skutterudite. Argentite appears with native silver at the Black Hawk but occurs after native silver in the Great Bear Lake area. The position of pitchblende is variable in the paragenetic sequence. At the Black Hawk, pitchblende coprecipitates with native silver. While at Great Bear, pitchblende occurs before silver. Dolomite (ankerite) is the predominant gangue mineral for this stage. The Black Hawk's sulphide stage is the equivalent of stages 5,6, and 7 for the Great Bear deposit. This period of mineral deposition is characterized by galena, chalcopyrite, sphalerite, argentite, and native silver. The predominant gangue mineral for this phase is dolomite with a late calcite phase. Von Barga (1979) describes other sulphides and sulphosalts but they occur in minor amounts only. The paragenesis for Cobalt-Gowganda area is similar to figures 13 and 14, however, there is a district-wide mineral zonation for the arsenide minerals; nickel arsenides are most abundant near the Nipissing diabase, followed by cobalt arsenides, and iron arsenides are present furthest away from the diabase. Kongsberg has a similar paragenesis (Segelstad, personal comm.) but native silver is the most

abundant constituent while the arsenide and sulphide phases are very minor.

ORE SHOOT GEOMETRY

The ore shoots for this type of deposit are generally high grade but low tonnage. They are a few millimeters to a meter wide and have strike lengths from a few millimeters to 100 meters. These shoots occur in steeply dipping veins and pinch and swell with barren zones between. Ore has been mined at Kongsberg, Norway to about 1000 meters depths with ore shoots separated by vertical barren zones of 30 meters (Ridge, 1984). Ore shoots in the Cobalt-Gowganda area extend up to 100 meters vertically (Petruk, 1971). Ore shoots at the Black Hawk as described earlier extend only 20 meters.

ALTERATION ASSEMBLAGES

Alteration minerals which characterize Ag-Ni-Co-As-U deposits are chlorite, sericite, hematite, and carbonate. These minerals generally occurs in a narrow margin flanking the vein. District-wide zoning and vertical changes are unclear from deposit to deposit. Alteration assemblages for these deposits are only briefly described but are comparable to that of the Black Hawk district.

Jambor (1971) describes the alteration at Cobalt-Gowganda to consist of three stages in a narrow band along the veins, each of which overlaps one another. These alteration stages are an albite-chlorite zone existing closest to the vein, which is followed by a carbonate-rich zone, and then a sericitic zone. Plagioclase feldspars are altered to sericite furthest away from the vein, which then grades to albite nearest the vein. Amphiboles and biotite aren't affected until the carbonate-rich phase, at which point they alter to chlorite and magnetite intergrowths. Pyroxenes dominate the alteration in the carbonate-rich zone by altering to carbonate and chlorite.

Critical Factors for the Formation of Ag-Ni-Co-As-U Type Deposits

The critical factors for the formation of Ag-Ni-Co-As-U type deposits are;

- 1) Their occurrence in Precambrian, calc-alkaline, batholithic complexes. This relationship is unclear but these rocks may be required as a source for the ore elements.

- 2) The close spatial association of the ore with a precursor sulphide stage. The sulphides probably act as a reducing agent and a source for sulfur.

3) The close spatial association of the ore with intrusives. The composition for the intrusive phase range from granitic to basic. The intrusive is the heat source for the hydrothermal system.

4) Mineralization always occurs in narrow, carbonate-filled, fissure veins. Therefore, faults and fractures are needed as conduits for the ore fluids and as a site for deposition.

5) Fluid inclusion Th for silver mineralization occurs at about 230 °C.

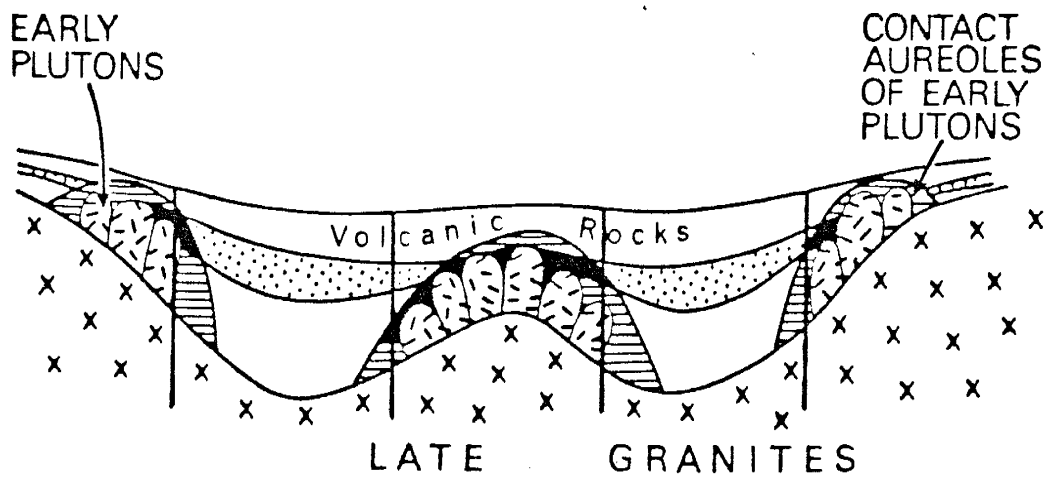
7) The pH of the fluids must be above 4 in order to deposit silver and carbonate minerals.


Genetic Theories

MAGMATICALLY DERIVED HYPOTHESIS


Badham (1975) proposes that this type of mineralization is the result of fluids from granitic magmas that intrude earlier, comagmatic volcanic-plutonic complexes at the close of an orogenic cycle. He points out that a probable place for deposition is in dilatant zones within fractured, sulphide-rich rocks around the margins of earlier intrusions (Fig. 15). Halls and Stumphl (1972) suggested that these deposits are derived from deep magmatic (?) fluids which leach the root zone of a mafic complex commonly associated

Figure 15. Magmatically derived model for the deposition of Ag-Ni-Co-As-U type deposits (Badham, 1975).



 Limit of areas at correct T & P for hydrothermal mineralisation at any particular time.

 Ideal sites for deposition of Ag-Arsenide.

 Probable sites of primary faults

with volcanism in a rift environment.

There is no association of Ag-Ni-Co-As-U deposits with any single type of intrusive rock as there is for example with Sn and Cu deposits, which are generally believed to be formed from magmatic fluids. Also a magmatic origin for the fluids is not supported by geochemical evidence. Robinson and Ohmoto (1973) and T. Segelstad (personal comm.) have concluded from isotope studies that the fluids, which these deposits were derived from, could not be magmatic but were either meteoric or connate waters.

CONTINENTAL WEATHERING HYPOTHESIS

Barbier (1974) proposes that vein-type U deposits, which includes the Ag-Ni-Co-As-U association, are derived from continental weathering. He believes that a prerequisite for these deposits is a source rock containing the needed metals. Fluids responsible for ore deposition are believed to be surface waters which descended to great depths and precipitated the ore by wallrock reactions.

Major evidence in opposition to this model is the geothermometry data available for these deposits. Fluid inclusion temperatures for these ore fluids are typically greater than 200 °C and are boiling. Needless to say this type of fluid would not be expected under normal continental weathering conditions.

EPITHERMAL FORMATION HYPOTHESIS

The model which agrees best with the available evidence for this class of deposit is that of an epithermal system similar to that proposed by Robinson and Ohmoto (1973). The basic ingredients for this model consists of a heated fluid, leaching of dissolved constituents in ore fluids from the country rocks, and precipitation of metals as the solution migrates towards the surface.

SUGGESTED GENETIC MODEL

The data presented here are consistent with the following sequence of events at the Black Hawk district. Intrusion of the Twin Peaks stock into a Precambrian batholithic complex occurred about 72 m.y. ago (Fig. 16). This intrusion produced fluids and created a large convective cell to circulate waters through fractures. It has been shown in many natural hydrothermal systems that a supercritical fluid can be formed from a cooling intrusive (Drummond, 1981). There are two pressure-temperature paths that a supercritical fluid may follow when separating from a cooling intrusive (Fig. 17). For both paths the fluid becomes immiscible along the liquid-vapor phase boundary at point C. Along A-C, a vapor phase separates from the more dense liquid by boiling but when the fluid follows B-C, a liquid phase is removed from the lighter vapor phase by condensation. Once the fluid intersects the liquid-vapor boundary, the solution will continue to rise and cool. This generating a low and high salinity fluid such as observed in the pre-ore stage (I) fluid inclusions.

Fluids can also be heated to a lesser degree so that it does not form a supercritical fluid as shown in figure 16. Such a fluid would not separate to form a low and high salinity fluid and it is this type of fluid that would appear to be responsible for the main ore stage of

Figure 16. Idealized model of ore deposition for the Black Hawk deposit. Meteoric water moved laterally and upward (arrows) underneath a volcanic terrain. Ore deposition (shaded area) occurs primarily in Precambrian rocks adjacent to Laramide intrusive.

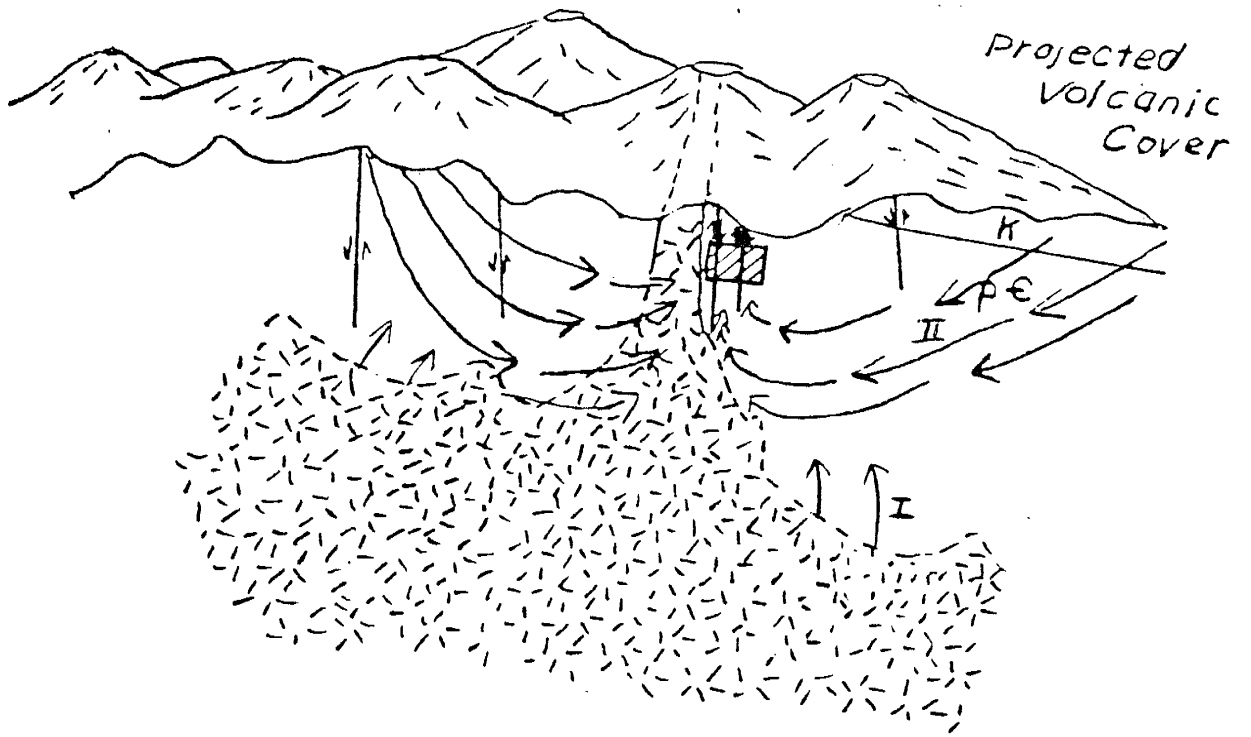
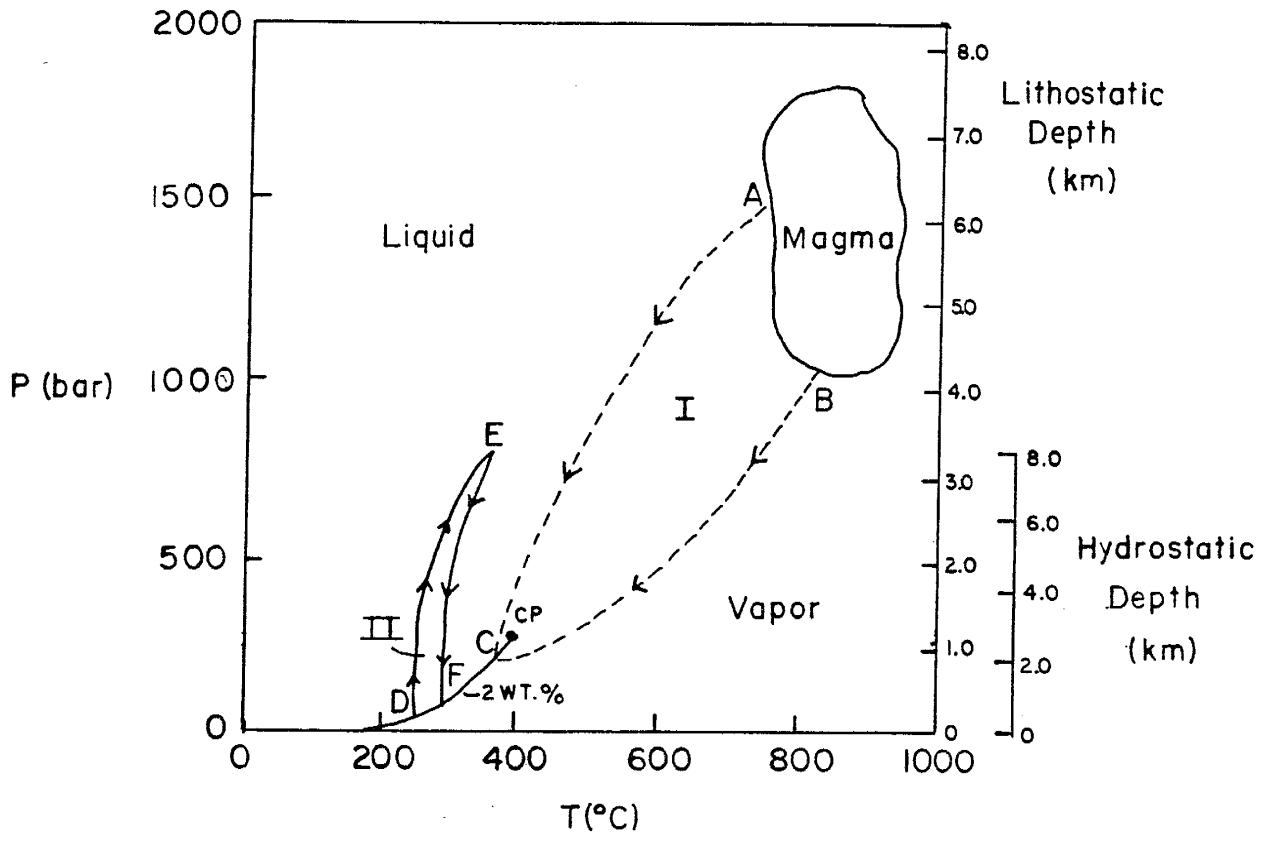


Figure 17. Pressure-temperature paths for hydrothermal systems. Refer to text for an explanation of the P-T paths (A-C, B-C, D-E-F; modified from Drummond, 1981).



mineralization (II). A temperature-pressure path for this fluid is depicted as D-E-F convective cell (Fig. 17). This fluid was heated by a heat source and rises along the path E-F. At point F, the fluid boils and moves along a path F-D. After cooling, the fluid descends along the path D-E and the process continues provided an adequate heat source exists. The absence of vapor-rich fluid inclusions in the main stage of mineralization indicates that mineral deposition occurred spatially below the level of boiling.

Fluid movement was channeled by the Laramide age, northeastern fracture systems both upward and laterally. The source of most ore fluid components (Ag, Ni, Co, As, U) is speculated to be primarily the country rocks. Data indicates that the metals were most likely transported by chlorine complexes (Barnes, 1979) and CO_3 complexes (Rich et al., 1977). Interaction of ore fluids and wallrocks resulted in the alteration of the original minerals to intermediate argillic assemblages nearest the vein with a propylitic alteration association decreasing in intensity away from the vein. Ore deposition occurred primarily in response to pH changes from wallrock reactions. The highest grade ore occurs in dilatant zones of fractured, sulphide-rich, porphyritic-monzodiorite gneiss near the margins of Twin Peaks intrusion.

SUMMARY AND CONCLUSIONS

Summary of the Geologic History
in the Black Hawk District

The geologic history of the study area includes metamorphism, igneous activity, sedimentation, and mineralization ranging from Proterozoic to Cretaceous time, as outlined below:

- 1) Formation of the Proterozoic Burro Mountain Batholith Complex. This complex includes the Bullard Peak and Ash Creek metamorphic series which were intruded by granites, porphyritic monzodiorite, and small isolated masses of anorthosite, diorite, and syenite.
- 2) Formation of northwest-trending fractures that crosscut the older Precambrian rocks and are then filled by diabase dikes.
- 3) Uplift and erosion of the Precambrian rocks followed by unconformable deposition of Cretaceous rocks.
- 4) Intrusion of rhyolite and granodiorite dikes.
- 5) Intrusion of the Laramide, Twin Peaks, diorite porphyry stock. The emplacement of this stock may have activated the northeast-trending faults and fractures and probably created the hydrothermal system responsible for the

Black Hawk mineralization.

6) Propylitic and intermediate-argillic alteration processes occurred along the northeast faults and fractures during the late stages or just after cooling of the Twin Peaks intrusive. A precursor sulphide stage consisting of pyrite and pyrrhotite is associated with the alteration.

7) Deposition of the Black Hawk mineralization. The paragenetic sequence is as follows: U + quartz; followed by Ag + (Ni, Co, Fe) arsenides + dolomite; and finally Bi + (Cu, Pb, Zn) sulphides + sulphosalts.

8) Emplacement of small andesite stocks during Cretaceous time.

9) Continued uplift and erosion during Cretaceous-Tertiary (?) times.

Conclusions

1) The Black Hawk district is located within a Proterozoic, subalkaline, calc-alkaline intrusive complex consisting primarily of monzodiorite and granite which is intruded by the Laramide Twin Peaks, diorite-porphyry stock. Monzodiorite gneisses contain approximately 35 ppm Co and 33 ppm Ni; the stock has approximately 20 ppm Co and 11 ppm Ni.

2) Ag-Ni-Co-As-U mineralization occurs in NE-trending, ankerite-bearing, fissure veins; mainly within the Proterozoic, porphyritic-monzoiorite gneiss and is spatially associated with the Twin Peaks intrusion.

3) Intermediate-argillic alteration developed along the vein, which resulted in the wallrock being enriched in H₂O, SiO₂, total Fe, MnO, MgO, and CaO and depleted in K₂O, Na₂O, and TiO₂. Propylitic alteration developed next away from the vein whereby the wallrock was enriched in H₂O, K₂O, and Na₂O and depleted in CaO, MnO, and total Fe. No distinction between barren and ore zones can be made on the basis of the associated alteration. K-Ar age for the intermediate-argillic alteration is 65.3 m.y..

4) Mineralization occurred at temperatures ranging from 410 to about 160 °C with salinities ranging from 0 to 40 eq.wt.% NaCl. Silver deposition is indicated to have occurred from fluids at temperatures at about 235 °C and salinities of 0 to 4 eq.wt.% NaCl.

5) Formation of the deposit probably resulted from the Twin Peaks intrusive as suggested by the close spatial and age relation between the mineralization and the intrusion.

6) The Black Hawk system formed in a subvolcanic environment at a depth of approximately 2.5 kilometers.

7) The Black Hawk district is similiar to many other Ag-Ni-Co-As-U type deposits (Kongsberg, Great Bear Lake, Cobalt-Gowganda area, etc.) in host rocks, ore mineralogy, style of deposition, and alteration. Age of deposition and mineral abundances are variable.

8) Data combined with other Ag-Ni-Co-As-U type deposits suggests that the critical factors for the formation of these deposits are their occurrence within Precambrian batholithic complexes within carbonate-filled fissure veins in sulphide-rich host rocks that are spatially associated with intrusives; and fluid temperatures of about 230 °C and a pH above 4.

9) Data suggests that the Black Hawk district was mineralized by an epithermal system during Laramide intrusive activity, but deposition occurred at greater depths and higher temperatures than is reported for typical epithermal deposits.

APPENDIX A

Whole-rock, XRF geochemistry for the various rock types within the Black Hawk district. Ni and Co analyses are by atomic absorption methods. Also presented are CIPW normative minerals. Sample locations are on Plate 1.

Rock type:	Quartz-Fine-grained ite monzodiorite		Porphyrific monzodiorite gneiss		Biotite monzo- diorite		Diorite	Syenite	Granite	Diabase	Rhynolite	Diorite porphyry		Granodiorite	Andesite																	
	111-1E 114-7E	719-1 719-5	715-8	113-6B	113-6A	712-7						609-8	112-1B			113-3D	111-1C	710-6	713-4	112-3	112-10	463-1	212-2	112-9	111-2A	112-7	114-12	721-5	721-3	721-4		
Sample No.	111-1E 114-7E	719-1 719-5	715-8	113-6B	113-6A	712-7	609-8	112-1B	113-3D	111-1C	710-6	713-4	112-3	112-10	463-1	212-2	112-9	111-2A	112-7	114-12	721-5	721-3	721-4									
Major Oxides (wt.%)																																
SiO2	69.48	50.64	53.02	55.11	54.3	54.9	55	55.24	47.34	52.99	48.74	47.17	47.72	77.88	73.6	45.26	48.05	75.88	76.6	61.96	64.4	64.52	64.28	61.57	62.77	64.08	62.87	57.89	54.66			
TiO2	.56	.99	.87	1.38	1.48	1.45	1.5	1.45	1.08	1.06	1.01	1.29	.43	.82	.08	1.09	1.25	.07	.12	.38	.33	.34	.38	.64	.58	.76	.69	.61	.71			
Al2O3	14	16.13	16.11	17.79	17.89	17.85	17.47	17.3	14.32	16.17	12.91	18.68	14.42	12.02	13.78	16.54	16.53	14.51	14.51	14.32	16.87	16.92	16.84	16.6	17.11	15.48	15.89	15.75	15.78			
Fe2O3	3.88	9.17	8.73	8.93	9.1	9.02	9.46	7.83	7.94	8.73	11.78	11.03	3.55	1.03	1.37	13.54	12.37	1.5	.87	4.09	4.21	4.18	4.32	6.47	4.71	5.67	5.45	5.79	6.15			
MnO	.05	.14	.14	.14	.16	.16	.17	.11	.37	.14	.21	.14	.01	.12	.04	.18	.17	.07	.02	.13	.13	.12	.14	.12	.08	.08	.09	.12	.12			
MgO	1.07	5.92	6.51	2.48	2.56	2.53	2.89	3.53	2.73	5.97	11.45	6.97	0	0	.3	7.55	6.5	.31	.39	1.33	.91	.9	1.14	2.19	1.29	2.25	1.78	3.32	1.98			
CaO	1.26	8.02	7.5	5.26	5.41	5.37	4.64	2.17	6.25	6.14	6.57	8.68	.26	.24	.69	9.49	9.31	.07	.11	4.56	5.26	5.29	4.36	5.25	4.12	2.3	4.15	6.78	8.1			
Na2O	2.07	3.28	3.41	4.11	4.04	4.08	4.03	4.77	2.6	3.08	2.45	3.09	.24	3.72	3.15	2.18	2.17	.53	.18	4.13	3.5	3.49	3.71	3.44	2.24	4.08	3.47	3.59	3.48			
K2O	4.62	2.14	2.26	2.48	2.6	2.57	2.8	3.56	1.9	2.54	1.59	.84	11.93	4.01	6.68	.74	1.63	4.08	3.85	2.04	2.06	2.32	2.16	3.08	4.08	3.27	2.27	2.43	2.43			
P2O5	.08	.24	.23	.37	.39	.42	.4	.37	.31	.19	.16	.19	.13	.04	.06	.33	.24	.02	.83	.22	.22	.21	.21	.21	.35	.29	.18	.17	.21	.22		
LOI	1.81	2.46	1.72	1.08	.8	.97	1.41	3.39	11.5	2.46	3.18	1.47	.41	.14	.37	1.73	1.59	2.29	2.52	4.87	2.1	2.31	2.42	1.35	3.37	1.17	1.21	2.76	5.73			
Total	98.88	99.15	100.5	99.13	98.73	99.32	99.77	99.64	94	99.47	100.85	99.75	99.1	99.22	100.12	99.23	99.81	99.33	99.2	100	99.99	100.34	100.1	100.16	99.68	100.33	99.03	99.06	99.36			
Minor Elements (ppm)																																
Ni	---	---	---	23	23	23	24	---	---	---	---	---	---	---	---	---	---	---	---	---	---	---	---	---	---	---	---	---	---	---	---	
Co	---	---	---	34	37	34	---	---	---	---	---	---	---	---	---	---	---	---	---	---	---	---	---	---	---	---	---	---	---	---	---	---
CIPM Normative Minerals (wt.%)																																
Q	36.55	0	0	4.56	3.3	4	3.94	3.5	22.22	1.65	0	0	28.77	40.81	28	0	0	58.33	62.08	19.44	24.03	24.17	23.15	17.87	28.19	16.28	18.47	10.77	8.03			
Or	28.18	13.18	13.61	15.05	15.8	15.55	16.95	21.98	13.72	15.58	9.8	5.1	71.51	23.88	39.53	4.54	9.92	24.83	23.51	12.7	12.46	12.39	14.07	12.98	18.95	24.41	19.82	13.99	15.41			
Ab	18.08	28.92	29.41	35.72	35.16	35.36	34.94	41.55	2.69	27.05	21.62	26.87	2.06	31.72	26.89	19.16	18.9	4.62	1.57	36.82	30.32	30.19	32.22	29.59	19.74	34.95	30.12	31.67	31.39			
An	5.91	23.93	22.4	23.39	23.46	23.33	20.91	8.72	35.41	23.66	20.37	36.13	.45	.94	3.04	34.44	31.45	.22	.36	21.04	24.82	24.99	20.79	23.86	19.31	10.36	18.59	21.01	21.73			
C	3.61	0	0	0	0	0	.34	2.77	1.48	0	0	0	.97	1.73	.26	0	0	9.42	10.25	0	0	0	.82	0	3.43	.81	0	0	0			
Di	0	12.82	11.34	.78	1.11	.94	0	0	5.41	10.12	5.6	0	0	0	10.06	11.95	0	0	1.03	.35	.36	0	.24	0	0	1.14	18.19	16.33	0	0		
Hv	3.39	8.15	14.29	13.95	14.17	14.03	16.1	13.92	10.46	21.09	17.07	2.15	0	.75	8.96	12.37	.8	1	4.43	3.88	3.78	4.74	10.45	5.52	7.63	7.13	7.63	1.81	0	0		
Pl	0	7.39	3.77	0	0	0	0	0	0	15.61	18.95	0	0	0	16.46	10.15	0	0	0	0	0	0	0	0	0	0	0	0	0	0	0	
Mt	2.99	3.02	2.96	2.98	2.98	2.97	2.97	3.79	2.66	3.01	3.02	2.24	1.84	0	0	2.26	2.24	0	0	3.06	2.97	2.97	2.98	2.95	3.02	3.67	3.02	3.11	0	0		
Hb	0	0	0	0	0	0	0	0	0	0	0	0	0	0	0	0	0	0	0	0	0	0	0	0	0	0	0	0	0	0		
Il	1.1	1.96	1.68	2.69	2.89	2.82	2.92	2.88	2.51	2.89	2	2.52	.83	0	0	3.33	2.44	0	0	.76	.64	.66	.74	1.24	1.15	1.46	1.34	1.21	1.45			
Ap	.19	.63	.54	.88	.93	1	.95	.9	.88	.46	.39	.45	.31	.09	.14	.79	.57	.05	.07	.54	.52	.5	.5	.92	.7	.42	.4	.51	.55			
Ne	0	0	0	0	0	0	0	0	0	0	0	0	0	0	0	0	0	0	0	0	0	0	0	0	0	0	0	0	0	0		

NOTE: Total iron reported as Fe2O3.

APPENDIX B

Petrographic descriptions for the whole-rock, geochemistry samples.

Rock type	Sample No.	Major minerals (%)	Minor minerals (%)	Texture	Comments
Quartzite	111-1E	Quartz(60), Alkali feldspar(30)	Mica(7), Magnetite, Epidote	granoblastic	
Fine-grained monzodiorite	111-70	Plagioclase(55), Hornblende(15), Alkali-feldspar(10), Biotite(10)	Quartz(2), Chlorite(2), Sericite(3), Epidote, Iron oxides, Apatite	fine-grain equigranular	sericitization of feldspar chloritization of biotite
Fine-grained monzodiorite	114-7E	Plagioclase(50), Hornblende(12), Alkali-feldspar(13), Biotite(10)	Quartz(3), Chlorite(3), Sericite(2), Epidote, Iron oxides, Apatite	fine-grain equigranular	sericitization of feldspar chloritization of biotite
Porphyritic monzodiorite	719-1	Plagioclase(65), Alkali-feldspar(10), Hornblende(10)	Biotite(6), Quartz(5), Sericite, Apatite, Iron oxides(2)	medium to coarse-grain porphyritic	slight sericitization of feldspar
Porphyritic monzodiorite	719-5	Plagioclase(65), Hornblende(10), Alkali-feldspar(10), Biotite(10)	Sericite, Apatite, Iron oxides(3), Quartz	medium to coarse-grain porphyritic	slight sericitization of feldspar
Porphyritic monzodiorite	715-8	Plagioclase(60), Biotite(12), Alkali-feldspar(15)	Hornblende(6), Quartz(3), Sericite, Apatite, Iron oxides(2)	medium to coarse-grain porphyritic	sericitization of feldspar
Porphyritic monzodiorite	113-68	Plagioclase(55), Hornblende(10), Alkali-feldspar(15)	Biotite(5), Quartz(5), Sericite(3), Chlorite, Apatite, Iron oxides(4)	medium to coarse-grain porphyritic	sericitization of feldspar chloritization of biotite
Biotite monzodiorite	720-4	Plagioclase(50), Biotite(15), Alkali-feldspar(15), Hornblende(10)	Sericite(3), Chlorite(2), Apatite, Quartz, Iron oxides(3)	medium-grain equigranular	slight sericitization of feldspar slight chloritization of biotite

Rock type	Sample No.	Major minerals (%)	Minor minerals (%)	Texture	Comments
Diorite	113-9A	Plagioclase(50), Hornblende(10), Chlorite(20)	Biotite(5), Alkali-feldspar(5), Sericite(6), Iron oxides(3), Apatite	medium-grain equigranular	sericitization of feldspar severe chloritization of mafic minerals
Diorite	712-7	Plagioclase(55), Hornblende(30)	Biotite(7), Alkali-feldspar(4), Iron oxides(3), Sericite, Chlorite	medium-grain equigranular	slight sericitization of feldspar slight chloritization of biotite
Syenite	609-8	Alkali-feldspar(70), Quartz(25),	Sericite(2), Iron oxides(2), Apatite	medium-grain	quartz is secondary, iron-oxide stained feldspars
Granite	112-1B	Alkali-feldspar(35), Quartz(32), Plagioclase(20)	Muscovite(5), Biotite, Iron oxides(3), Apatite, Zircon	pegmatitic	
Granite	113-3D	Alkali-feldspar(50), Quartz(28), Plagioclase(15)	Biotite(3), Iron oxides(2), Apatite, Zircon	medium-grain equigranular	
Diabase	111-1C	Plagioclase(60), Pyroxene(32)	Iron oxides(5), Sericite, Chlorite(2)	very fine-grain subophitic	slight sericitization of feldspar slight chloritization of pyroxene
Diabase	710-6	Plagioclase(57), Pyroxene(30)	Iron oxides(7), Chlorite(3), Sericite, Calcite	very fine-grain subophitic	carbonatization and sericitization of feldspar
Rhyolite	713-4	Quartz(65), Alkali-feldspar(10)	Iron oxides(2)	fine-grain	silicification severe sericitization of feldspar
Rhyolite	112-3	Quartz(60), Sericite(25), Alkali-feldspar(11)	Iron oxides(4)	fine-grain	quartz veinlets, severe sericitization of feldspar
Diorite porphyry	112-10	Cryptocrystalline groundmass(65), Plagioclase(20), Quartz(10)	Hornblende(2), Calcite, Sericite(2), Iron oxides	fine to medium-grain porphyritic	carbonatization and sericitization of feldspars
Diorite porphyry	603-1	Cryptocrystalline groundmass(60), Plagioclase(29)	Alkali-feldspar(3), Hornblende(4), Iron oxides(2), Sericite, Biotite	porphyritic	slight sericitization of feldspars

Rock type	Sample No.	Major minerals (%)	Minor minerals (%)	Texture	Comments
Diorite porphyry	212-2	Cryptocrystalline groundmass(65), Plagioclase(25)	Alkali-feldspar(2), Hornblende(3), Biotite, Iron oxides(3), Sericite	porphyritic	slight sericitization of feldspars
Diorite porphyry	112-9	Cryptocrystalline groundmass(63), Plagioclase(27)	Alkali-feldspar(4), Hornblende(3), Sericite, Iron oxides(2)	porphyritic	slight sericitization of feldspars
Diorite porphyry	111-2A	Cryptocrystalline groundmass(60), Plagioclase(25)	Alkali-feldspar(2), Hornblende(5), Sericite(3), Iron oxides(3), Biotite	porphyritic	sericitization of feldspars
Granodiorite	112-7	Plagioclase(50), Quartz(22), Alkali-feldspar(10), Hornblende(10)	Chlorite(2), Sericite(2), Iron oxides(3), Epidote	fine-grain equigranular	sericitization of feldspars chloritization of biotite epidote veinlets
Granodiorite	114-12	Plagioclase(55), Quartz(20), Alkali feldspar(10), Hornblende(11),	Sericite, Iron oxides(3)	fine-grain equigranular	sericitization of feldspars
Granodiorite	721-5	Plagioclase(60), Quartz(21), Alkali-feldspar(12)	Hornblende(4), Sericite, Iron oxides(2)	fine-grain equigranular	slight sericitization of feldspars
Andesite	721-3	Cryptocrystalline groundmass(70), Plagioclase(20)	Hornblende(3), Biotite(3), Iron oxides(3), Sericite	porphyritic	sericitization and carbonatization of feldspars
Andesite	721-4	Cryptocrystalline groundmass(65), Sericite	Hornblende, Chlorite(3), Plagioclase(8), Calcite(2), Alkali-feldspar(2), Iron oxides(4), Biotite,	porphyritic	sericitization and carbonatization of feldspars chloritization of mafic minerals

APPENDIX C

Fluid inclusion data and sample locations. Alh 1, Alh 2, Alh 3 are high grade samples.

Sample Number	Location	Incls. type	Filling Temperature (C)			Salinity (eq. wt. % Na Cl)		
			No. incls	Temp. range	Mean temp.	No. incls.	Saln. range	Mean Saln.
617-4a	Lv.11, 80'	II	7	155-388	301.14	2	0-2.06	1.03
*	SW of raise	III	7	317-392	371.14	4	0-2.40	.69
617-4b	Lv.11, 80'	II	3	201-235	216.00	3	3.37-5.10	4.05
**	SW of raise							
211-11	Lv.11, 50'	II	14	160-385	341.00	3	0-2.56	.85
*	SW of raise	III	4	350-404	389.50	-	-----	---
615-12a	Lv.11, 80'	II	4	335-390	372.75	2	0.00	0.00
*	SW of raise	III	5	389-401	395.60	-	-----	---
		IV	2	323-330	326.50	2	39.60-39.65	39.63
615-12b	Lv.11, 80'	II	2	260-351	306.00	1	2.56	2.56
**	SW of raise	III	1	375	375.00	-	-----	---
211-2	Lv.3, main shaft	II	6	299-389	330.67	-	-----	---
*		III	2	398-399	398.50	2	1.39	1.39
211-4	Lv.6, 200'	II	7	163-210	188.00	-	-----	---
***	NE of shaft							
Alh 1	unknown	II	14	81-255	209.55	7	.52-2.40	1.41
**								
Alh 2	unknown	II	11	190-280	251.00	7	1.39-2.40	1.70
**								
Alh 3	unknown	II	12	190-280	219.33	6	.70-2.06	1.49
**		III	1	278	278.00	-	-----	---

NOTE: Samples from the Black Hawk mine; 617-4, 211-11, 615-12, 211-2, 211-4
Samples from the Alhambra mine; Alh 1, Alh 2, Alh 3.

* indicates samples from Pre-ore stage
** indicates samples from Main stage
*** indicates samples from Late stage.

REFERENCES

- Badham, J.P.N., 1976, Orogenesis and metallogenesis with reference to the Ag-Ni-Co-As ore association, in Strong, D.F. (ed.), Metallogeny and plate tectonics: Geological Association of Canada Special Paper no. 14, 559-571.
- , 1975, Mineralogy, paragenesis, and origin of the Ag, Ni, Co arsenide mineralization, Camdsell River, N.W.T., Canada: Mineralium Deposita, v. 10, 153-175.
- Barbier, J., 1974, Continental weathering as a possible origin of vein-type uranium deposits: Mineralium Deposita, v. 9, 271-288.
- , 1978, Magnetite-Apatite-Amphibole-Uranium and Silver-Arsenic mineralization in L. Proterozoic igneous rocks, East Arm, Great Slave Lake, Canada: Economic Geology, v. 73, 1474-1491.
- Barnes, H.L., 1979, Geochemistry of Hydrothermal Ore Deposits, 2nd ed.: John Wiley and Son Inc., New York, 798pp.
- Bastin, E.S., 1939, The nickel-cobalt-native silver ore type: Economic Geology, v. 34, 1-40.
- Bowden, P., 1985, The geochemistry and mineralization of alkaline ring complexes in Africa (a review): Journal of African Earth Sciences, v. 3, 17-39.
- Boyle, R.W. and Daas, A.S., 1971, Origin of native silver at the Cobalt, Canada deposits: Canadian Mineralogist, v. 11, 414-417.
- Branvold, L.A., 1974, Atomic absorption methods for analysis of some elements in ores and concentrates: New Mexico Bureau of Mines and Mineral Resources Circular, no. 142, 22pp.
- Buddington, A.F., 1959, Granite emplacement with special reference to North America: Geological Society of America Bulletin, v. 70, 671-747.
- Cox, K.G., Bell, J.D., and Pankhurst, R.J., 1979, The Interpretation of Igneous Rocks : George Allen and UNWIN LTD., London, 450p.

- Drummond, S.E., 1981, Boiling and mixing of hydrothermal fluids: chemical effects on mineral precipitation, PH.D. dissertation from Pennsylvania State University: University Microfilm International, no. 81127798.
- Elston, W.E. and Northrop, S.A., 1976, Cenozoic Volcanism in Southwestern New Mexico: New Mexico Geological Society Special Paper no. 5.
- Gammon, J.B., 1966, Fahlbands in the Precambrian of southern Norway: Economic Geology, v. 61, 174-188.
- Gillerman, E. and Whitebread, K.H., 1956, Uranium-bearing nickel-cobalt-native silver deposits, Black Hawk district, Grant County, New Mexico: U.S.G.S. Bulletin 1009-K, 283-313 illus. incl. geol. map.
- , 1964, Mineral deposits of Western Grant County, New Mexico: New Mexico Bureau of Mines and Research, Bulletin, no. 83.
- Haas, J.L., 1971, The effect of salinity on the maximum thermal gradient of a hydrothermal system at hydrostatic pressure: Economic Geology, v. 66, 940-946.
- Hall, C. and Stumpf, F.R., 1972, The five-element (Ag-Bi-Co-Ni-As) - A critical appraisal of the geological environment in which it occurs and of the theories affecting its origin (abs.): 24th International Geological Congress, Section 4, 540.
- Hedlund, D.C., 1978, Geologic map of Wind Mountain quadrangle, Grant County, New Mexico, scale 1:24,000: U.S.G.S. Miscellaneous Field Studies Map, no. 1031.
- , 1980, Geologic Map of the Redrock NE quadrangle, New Mexico, scale 1:24,000: U.S.G.S. Miscellaneous Field Studies Map, no. 1264.
- Heidrick, T.L. and Titley, S.R., 1982, Fracture and dike patterns in Laramide plutons and their structural and tectonic implications: in Titley, (ed.), Advances in Geology of the Porphyry Copper Deposit: The University of Arizona Press, Tucson, Arizona.
- Hewitt, C.H., 1959, Geology and mineral deposits of the northern Big Burro Mountains, Grant County, New Mexico: New Mexico Bureau of Mines and Research, Bulletin, no. 60, 151pp.

- Irvine, T.N. and Baragar, W.R.A., 1971, A guide to the chemical classification of the common volcanic rocks: Canadian Journal of Earth Sciences, v. 8, 523-548.
- Jambor, J.L., 1971, General geology; the silver-arsenide deposits of the Cobalt-Gowganda region, Ontario: Canadian Mineralogist, v. 11, 12-34.
- Kerr, P.F., 1977, Optical Mineralogy: McGraw-Hill Inc., New York, 492p.
- Kolessar, 1983, The Tyrone Copper Deposit: in Titley, (ed.), Advances in Geology of the Porphyry Copper Deposit: The University of Arizona Press, Tucson, Arizona, 327-333.
- Knipping, H.D., 1974, The concepts of supergene vs. hypogene emplacement of U at Rabbit Lake, Saskatchewan, Canada: Formation of U Ore Deposits, International Atomic Energy Agency, Vienna, 531-549.
- Krauskopf, K.B., 1979, Introduction to Geochemistry, 2nd ed.: McGraw-Hill Inc., New York, 617p.
- Langford, F.F., 1974, A supergene origin for vein type uranium ores in the light of the Western Australian calcrete-carnotite deposits: Economic Geology, v. 69, 516-526.
- Leach, A.A. 1916, Black Hawk silver-cobalt ores : Engineer and Mine Journal, v. 102, 456.
- Le Maitre, R.W., 1976, The chemical variability of some common igneous rocks: Journal of Petrology, v. 17, 589-637.
- Lindgren, W., 1933, Mineral Deposits: McGraw-Hill, Inc., New York, 930p.
- Naumov, G.B., Motorina, Z.M., and Naumov, V.B., 1971, Conditions of formation of carbonates in veins of the Pb-Co-Ni-Ag-U type: Geochemistry International, v. 6, 76-107.
- Norrish, K. and Hutton, J.T., 1969, An accurate X-ray spectrographic method for the analysis of a wide range of geologic samples: Geochimica et Cosmochimica Acta, v. 33, 431-453.
- Petruk, W., 1971, General characteristics of the deposits; The silver-arsenide deposits of the Cobalt-Gowganda region, Ontario: Canadian Mineralogist, v.11, 76-107.

- Potter, II, R.W., Babcock, R.S., and Brown, D.L., 1977, A new method for determining the solubility of salts in aqueous solutions at elevated temperatures: *Journal of Research, U.S. Geological Survey*, v. 5, 389-395.
- Rich, R.A. and Holland, H.D., 1977, *Hydrothermal Uranium Deposits*: Elsevier Scientific, Inc., New York.
- Ridge, J.D., 1984, *Annotated Bibliographies of Mineral Deposits in Europe*: Pergammon Press, New York.
- Robinson, B.W. and Ohmoto, H., 1973, Mineralogy, fluid inclusions, and stable isotopes of the Echo Bay U-Ni-Ag-Cu deposits, N.W.T.: *Economic Geology*, v. 68, 635-656.
- Roedder, E.W., 1972, *Composition of fluid inclusions*: U.S.G.S., Professional Paper, 440 JJ.
- , 1984, *Fluid Inclusions: Mineralogical Society of America's Reviews in Mineralogy*, v. 12.
- Ruzicka, V., 1971, Geological comparison between East European and Canadian Uranium deposits: *Geological Survey of Canada, Paper 70-48*
- Scott, S.D. and O'Connor, T.P., 1971, Fluid inclusions in vein quartz, Silverfields mine; The silver-arsenide deposits of the Cobalt-Gowganda region, Ontario: *Canadian Mineralogist*, v. 11, 263-271.
- Sillitoe, R.H. and Bonham, H.F. Jr., 1984, Volcanic landforms and ore deposits: *Economic Geology*, v. 79, no. 6, 1286-1298.
- Sourirajan, S. and Kennedy, G.C., 1962, The system H₂O-NaCl at elevated temperatures and pressures: *American Journal of Science*, v. 260, 115-141.
- Stacey, J.S. and Hedlund, D.C., 1983, Lead-isotopic compositions of diverse igneous rocks and ore deposits from southwestern New Mexico and their implications for early Proterozoic crustal evolution in the western United States: *Geological Society of America Bulletin*, v. 94, 43-57.
- Streckieson, A.L., 1973, Plutonic rock classification and nomenclature recommended by the IUGS subcommission on the systematics of igneous rocks: *Geotimes*, v. 18, 26-30.

Turekian, J.A. and Wedepohl, K.H., 1961, Distribution of the elements in some major units of the earth's crust: Geological Society of America Bulletin, v. 72, 175-192.

Von Bargaen, D.J., 1979, The Silver-Antimony-Mercury System and The Mineralogy of The Black Hawk District, New Mexico (PhD. thesis): Purdue University, 226p.

This thesis is accepted on behalf of the faculty
of the Institute by the following committee:

Donald L. Norman

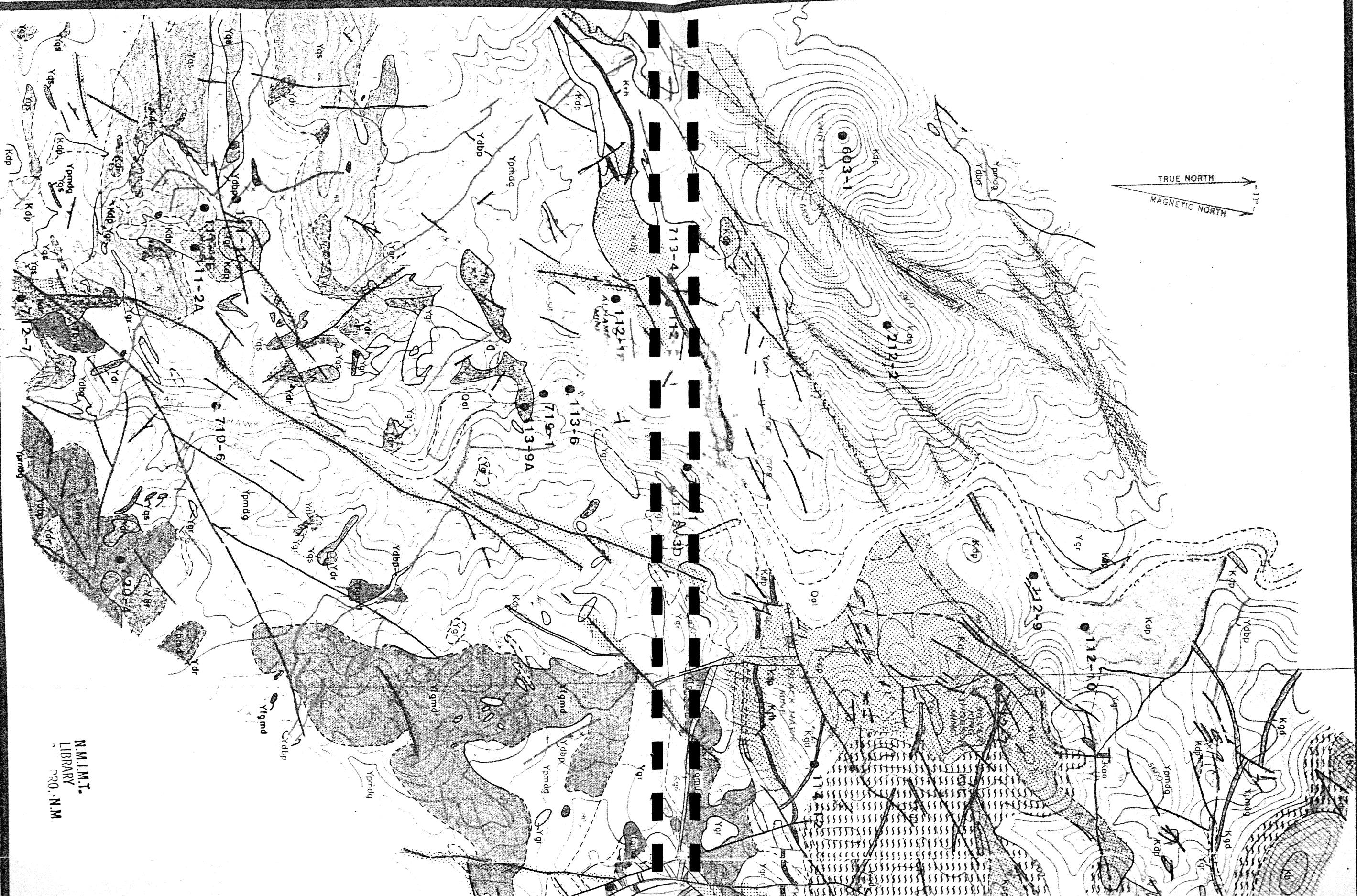
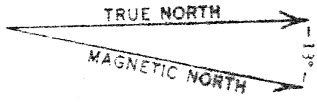
Advisor

James M. Roberts

Glenn R. Shea

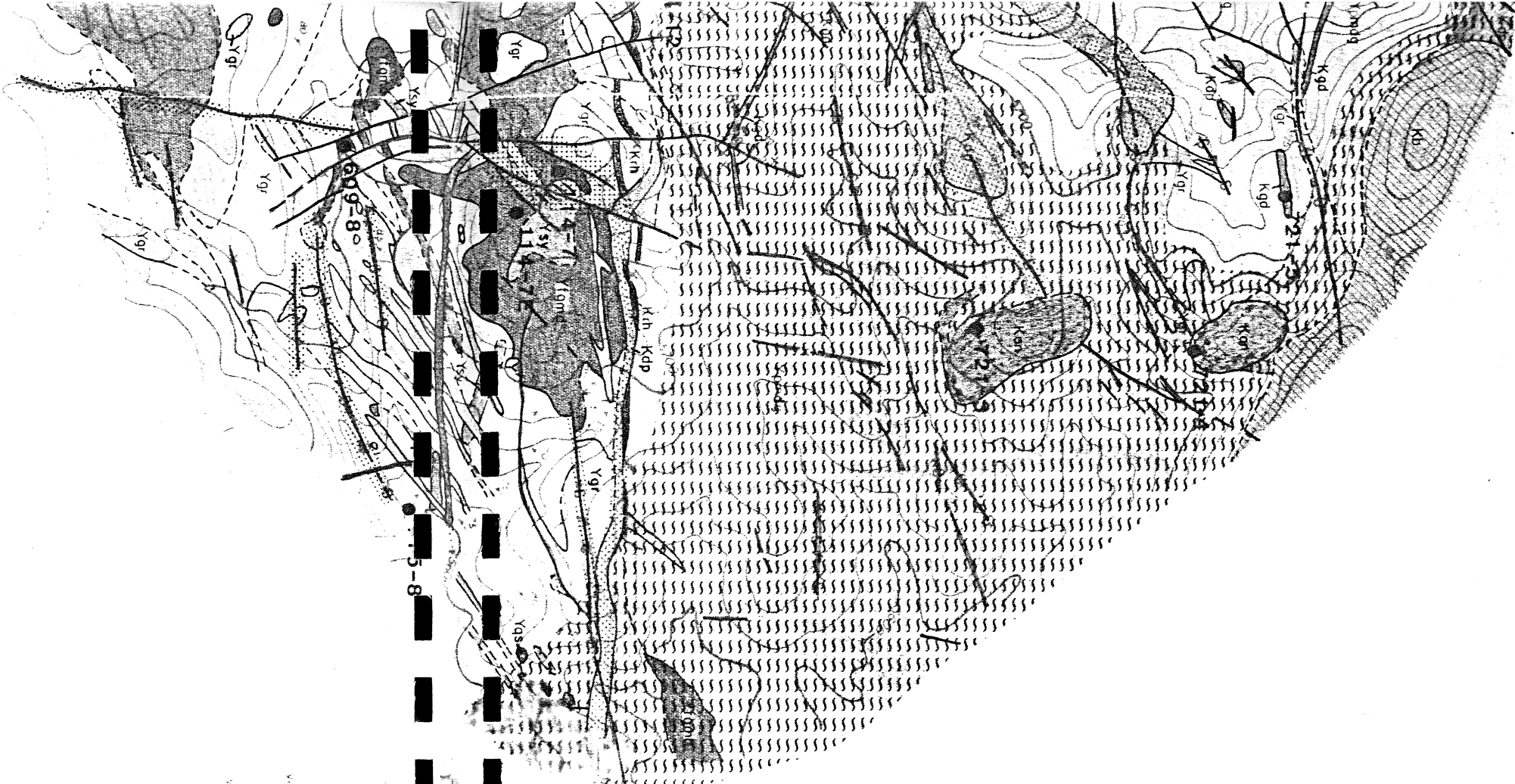
22 April 1986

Date



GEOLOGIC MAP OF THE BLACK HAWK MINING DISTRICT.

N.M.M.T.
LIBRARY
700 N.M.



EXPLANATION

SEDIMENTARY ROCKS

Ool Alluvium

Kb Berooth quartzite

Kah Andesite

Kgd Granodiorite

Kdp Diorite porphyry

Krh Rhyolite

Ydgp Diabase and basalt porphyry

Ygr Granite

Ysy Syenite

Ydr Diorite

Ybnd Biotite monzodiorite

Ydgp Porphyritic monzodiorite gneiss

Ybnd Grained monzodiorite

Ydgp Quartzite and schist

CRETACEOUS QUATERNARY

CRETACEOUS PROTEROZOIC

ALTERATION

Paleoregolith ?

Propylitic and/or Intermediate or gneissic

N.M.

DISTRICT, GRANT COUNTY, NEW MEXICO

Geology modified after Gillerman and Whitebread, 1956
 Alteration by J.E. Gerwe, 1985